TURUN
YLIOPISTO
UNIVERSITY
OF TURKU

Interactions Between Tannins and Anthelmintics – Molecular Aspects and Mechanisms

Mimosa Sillanpää

TURUN YLIOPISTON JULKAISUJA – ANNALES UNIVERSITATIS TURKUENSIS
SARJA – SER. AI OSA – TOM. 745 | ASTRONOMICA – CHEMICA – PHYSICA – MATHEMATICA | TURKU 2025

TURUN
YLIOPISTO
UNIVERSITY
OF TURKU

INTERACTIONS BETWEEN TANNINS AND ANTHELMINTICS – MOLECULAR ASPECTS AND MECHANISMS

Mimosa Sillanpää

TURUN YLIOPISTON JULKAISUJA – ANNALES UNIVERSITATIS TURKUENSIS
SARJA – SER. AI OSA – TOM. 745 | ASTRONOMICA – CHEMICA – PHYSICA – MATHEMATICA | TURKU 2025

University of Turku

Faculty of Science
Department of Chemistry
Chemistry
Doctoral Programme in Exact Sciences (EXACTUS)

Supervised by

Adjunct professor, Maarit Karonen
Department of Chemistry
University of Turku
Turku, Finland

Dr, Marica Engström
Institute of Biomedicine
University of Turku
Turku, Finland

Adjunct professor, Petri Tähtinen
Department of Chemistry
University of Turku
Turku, Finland

Reviewed by

Professor, Francisco A. Macías
Institute of Biomolecules (INBIO)
University of Cádiz
Cádiz, Spain

Research Professor, Antti Oksanen
Finnish Food Authority
Oulu, Finland

Opponent

Research Director, Carine Le Bourvellec
National Research Institute for Agriculture, Food and Environment (INRAE)
Avignon, France

ISBN 978-952-02-0275-0 (PRINT)
ISBN 978-952-02-0276-7 (PDF)
ISSN 0082-7002 (Print)
ISSN 2343-3175 (Online)
Painosalama, Turku, Finland 2025

UNIVERSITY OF TURKU
Faculty of Science
Department of Chemistry
Chemistry
MIMOSA SILLANPÄÄ: Interactions Between Tannins and Anthelmintics – Molecular Aspects and Mechanisms
Doctoral Dissertation, 173 pp.
Doctoral Programme in Exact Sciences
August 2025

ABSTRACT

Plant tannins have been widely studied for their antiparasitic properties. They also possess other beneficial effects for animal health and environment, such as controlling ruminant bloating and reducing the emission of greenhouse gases from the rumination process. Combined with commercial anthelmintics, tannins could offer a new type of strategy to control the development of anthelmintic resistance. However, more information on the interactions between tannins and commercial anthelmintics is needed as in vivo, different tannin-rich forages have demonstrated either synergistic or antagonistic effects when combined with oral anthelmintics, depending on the types of tannins and the analytical approaches involved.

In this work, the interactions of two tannin classes, proanthocyanidins (PAs) and hydrolysable tannins (HTs), with commercial anthelmintics were studied utilizing isothermal titration calorimetry (ITC) and nuclear magnetic resonance (NMR) spectroscopy. ITC studies were conducted using one commercial anthelmintic, thiabendazole (TBZ), while the NMR studies included two anthelmintics, TBZ and ivermectin. The ITC studies indicated that the strength of the interaction is greatly affected by the structural characteristics of tannins, the strongest interactions arising from the presence of galloyl groups and increased molecular weight of the tannin. In general, stronger interactions with TBZ were observed for PAs than for HTs of the same molarity. The results from the NMR study supported the information gained from ITC and in addition elucidated the molecular mechanisms of the interactions.

Differences in the interaction mechanisms were observed for the tannin classes studied, aligning with the in vivo findings on the effect of forage composition. The structural features of tannins involved in the interactions with commercial anthelmintics also contribute to the anthelmintic effects of tannins. This necessitates further research on the possible implications on the bioavailability of commercial anthelmintics if structurally the most potent tannins are used in combination with anthelmintics used as oral drenches

KEYWORDS: anthelmintic resistance, hydrolysable tannin, isothermal titration calorimetry, NMR spectroscopy, plant tannin, proanthocyanidin, tannin-anthelmintic interaction

TURUN YLIOPISTO
Matemaattis-luonnontieteellinen tiedekunta
Kemian laitos
Kemia
MIMOSA SILLANPÄÄ: Tanniinien ja loislääkkeiden väliset vuorovaikutukset – Molekulaariset näkökulmat ja vuorovaikutusmekanismit
Väitöskirja, 173 s.
Eksaktien tieteiden tohtoriohjelma
Elokuu 2025

TIIVISTELMÄ

Tanniinit ovat kasvien tuottamia erikoistuneita metaboliitteja, joilla on muun muassa havaittu olevan antiparasiittisia ominaisuuksia. Tanniinien on havaittu myös auttavan märehtijöiden pötsihäiriöiden hallinnassa sekä vähentävän märehtimisprosessissa syntyvien kasvihuonekaasupäästöjen määrää. Yhdistettyinä kaupallisten loislääkkeiden kanssa tanniinit voisivatkin tarjota uudenlaisen lähestymistavan loislääkeresistanssin kehittymisen hallitsemiseksi. Lisää tietoa tanniinien ja kaupallisten loislääkkeiden välisistä vuorovaikutuksista kuitenkin tarvitaan, sillä in vivo -tutkimuksissa on saatu ristiriitaisia tuloksia tanniinipitoisten rehujen vaikutuksesta annetun loislääkkeen tehoon, rehujen tanniinikoostumuksesta sekä tutkimuksissa käytetyistä analyysimenetelmistä riippuen.

Tässä työssä tutkittiin kahden tanniiniluokan, proantosyanidiinien (PA) ja hydrolysoituvien tanniinien (HT), vuorovaikutuksia kaupallisten loislääkkeiden kanssa. Tutkimusmenetelminä käytettiin isotermistä titrauskalorimetriaa (ITC) sekä ydinmagneettista resonanssispektroskopiaa (NMR). ITC:llä tutkittiin edellä mainittujen tanniiniluokkien vuorovaikutuksia tiabendatsolin (TBZ) kanssa, kun taas NMR:llä tutkittiin tanniinien vuorovaikutuksia kahden eri luokan loislääkkeen, TBZ:n ja ivermektiinin, kanssa. Kalorimetrialla saatujen tulosten perusteella voitiin yhdistää tanniinien rakenteelliset ominaisuudet havaitun vuorovaikutuksen voimakkuuteen; esimerkiksi tanniinirakenteen galloyyliryhmät sekä yhdisteen suurempi molekyylipaino kasvattivat vuorovaikutuksen suuruutta. Yleisesti ottaen PA:t osoittivat voimakkaampia vuorovaikutuksia TBZ:n kanssa kuin HT:t samassa konsentraatiossa. NMR-tulokset taas tukivat ITC-tutkimusten tuloksia sekä paljastivat lisää tietoa vuorovaikutusmekanismeista.

Eroja vuorovaikutuksissa havaittiin tanniiniluokkien välillä, mikä vastaa aiempia in vivo -tuloksia rehun koostumuksen vaikutuksesta loislääkkeen biologiseen hyötyosuuteen. Koska samat tanniinien rakenteelliset tekijät osallistuvat vuorovaikutuksiin niin loisten kuin loislääkkeiden kanssa, lisätutkimusta tarvitaan tanniinien vaikutuksesta loislääkkeiden biologiseen hyötyosuuteen, jos rakenteellisesti aktiivisimpia tanniineja aiotaan käyttää loislääkkeiden rinnalla.

ASIASANAT: hydrolysoituva tanniini, isoterminen titrauskalorimetria, kasvitanniini, loislääkeresistanssi, NMR-spektroskopia, proantosyanidiini, tanniini-loislääke-vuorovaikutus

Table of Contents

Abbreviations

AR	Anthelmintic resistance
BZ	Benzimidazole
COSY	Correlation spectroscopy
CYP	Cytochrome P450
DAD	Diode array detector
DHHDP	Dehydrohexahydroxydiphenoyl
DMSO	Dimethyl sulfoxide
ET	Ellagitannin
GIN	Gastrointestinal nematode
HESI	Heated electrospray ionization
HHDP	Hexahydroxydiphenoyl
HMBC	Heteronuclear multiple bond correlation
HPLC	High-performance liquid chromatography
HRF	Heterocyclic ring fission
HSQC	Heteronuclear single quantum coherence
HT	Hydrolysable tannin
ITC	Isothermal titration calorimetry
IVM	Ivermectin
mDP	Mean degree of polymerization
ML	Macrocyclic lactone
MRM	Multiple reaction monitoring
MS	Mass spectrometry
MS/MS	Tandem mass spectrometry
NHTP	Nonahydroxytriphenoyl
NMR	Nuclear magnetic resonance
PA	Proanthocyanidin
PC	Procyanidin
PD	Prodelphinidin
P-gp	P-glycoprotein
PTFE	Polytetrafluoroethylene
QM	Quinone-methide

RDA	Retro-Diels-Alder
ROESY	Rotating-frame nuclear Overhauser effect spectroscopy
SEM	Scanning electron microscopy
TBZ	Thiabendazole
TEM	Transmission electron microscopy
UHPLC	Ultrahigh-performance liquid chromatography

Artificial intelligence (ChatGPT, version GPT-4, OpenAI, San Francisco, CA, USA) was used as a language support tool and for data visualization during the writing process of this thesis.

List of Original Publications

This dissertation is based on the following original publications, which are referred to in the text by their Roman numerals I–III:

I **Sillanpää, M.**; Engström, M.T.; Tähtinen, P.; Green, R.J.; Käpylä, J.; Näreaho, A.; Karonen, M. Tannins Can Have Direct Interactions with Anthelmintics: Investigations by Isothermal Titration Calorimetry. *Molecules*, 2023, 28, 5261.

II **Sillanpää, M.**; Engström, M.T.; Tähtinen, P.; Green, R.J.; Käpylä, J.; Näreaho, A.; Karonen, M. Exploring the Interactions between Plant Proanthocyanidins and Thiabendazole: Insights from Isothermal Titration Calorimetry. *Molecules*, 2024, 29, 3492.

III **Sillanpää, M.**; Tähtinen, P.; Karonen, M. Molecular Aspects of Tannin–Anthelmintic Interactions as Revealed by NMR spectroscopy. *ACS Omega,* 2025, 10, 29, 32174–32188.

List of related publications not included in the thesis:

Suominen, E.; Savila, S.; **Sillanpää, M.**; Damlin, P.; Karonen, M. Affinity of Tannins to Cellulose: A Chromatographic Tool for Revealing Structure-Activity Patterns. *Molecules*, 2023, 28, 5370.

1 Introduction

Plants produce an extensive variety of different compounds for their growth and reproduction. Of these, plant tannins and other polyphenols play, for example, an important part as defensive compounds against various stressors, such as pathogens, herbivores, and UV radiation. Tannins can be divided into three sub-groups: proanthocyanidins (PAs, syn. condensed tannins), hydrolysable tannins (HTs), and phlorotannins. Of these, PAs and HTs, found widely in the plant kingdom, exhibit significant structural variability and have been compounds of interest for their bioactivities and their potential applications in various research areas, such as in agriculture and both human and animal health.[1–6] One of the most well-studied bioactivity of tannins is their affinity to proteins[7], but they have also been studied to act as antioxidants[8–10] and possess affinity to other biomolecules as well, such as lipids[11,12] and polysaccharides[13,14]. These bioactivities are linked, for example, to the abilities of tannins to act as antimicrobial[15,16] and antiparasitic[17–20] agents. The abundance and the ubiquitous nature of tannins make them potential candidates in new nematode control strategies. They can be found in nature, directly grown as forage or acquired from the by-products of the wood industry. Some examples of tannin-rich plants found in the Finnish nature are shown in Figure 1.

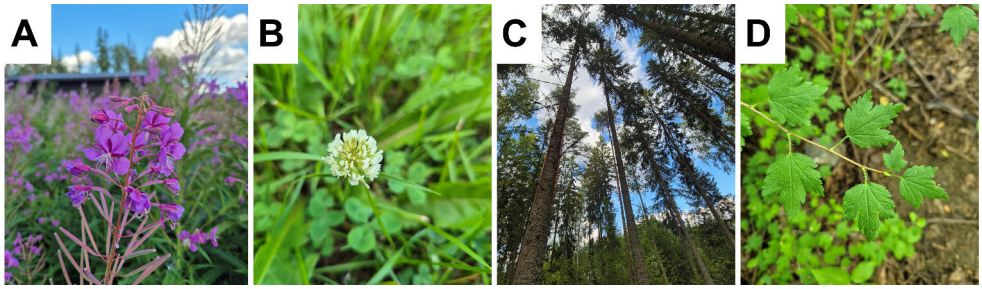

Figure 1. Examples of tannin-rich plants found in the Finnish nature. (**A**) Willowherb (*Chamaenerion angustifolium*), (**B**) white clover (*Trifolium repens*), (**C**) Scots pine (*Pinus sylvestris*), and (**D**) alpine currant (*Ribes alpinum*).

HTs are formed around a cyclic or acyclic polyol core, usually glucose. This central polyol can be further decorated with a variable number of esterified variants

of galloyl groups (Figure 2A). HTs can be divided into simple gallic acid derivatives, gallotannins, and ellagitannins (ETs). Simple gallic acid derivatives have one to five gallic acid moieties most commonly esterified directly to a glucose or quinic acid core, while gallotannins contain additional galloyl groups bound by depside bond to these galloyl groups. The structurally characteristic feature of ETs is the hexahydroxydiphenoyl (HHDP, Figure 2A) group formed of two galloyl moieties linked via oxidative coupling. The structural diversity of ETs is further amplified by the modifications of the HHDP group through oxidation and/or hydrolysis. These different varieties of HHDPs contain, for example, nonahydroxytriphenoyl (NHTP) and dehydrohexahydroxydiphenoyl (DHHDP) groups. Additionally, ETs can have different conformations of the glucose moiety, $^{1}C_4$ or $^{4}C_1$, and the moiety can be in a cyclic or acyclic form. These monomeric units can form intermolecular linkages, forming oligomers and polymers. The linkage types further increase the structural diversity of ETs, as the monomers can be linked to each other via five different types of linkages: GOG (dehydrodigalloyl), DOG (valoneoyl), GOD (sanguisorboyl), D(OG_2) and *C*-glucosidic, where G stands for galloyl, O for oxygen and D for HHDP.[21]

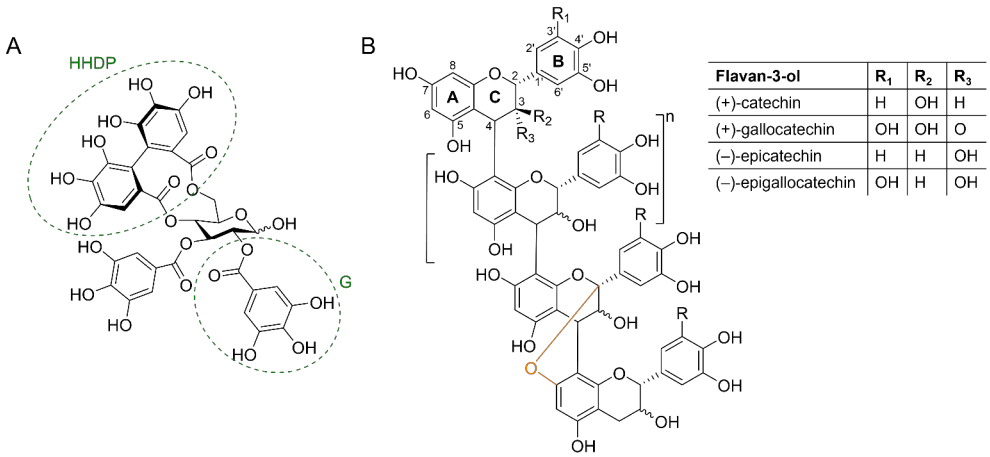

Flavan-3-ol	R_1	R_2	R_3
(+)-catechin	H	OH	H
(+)-gallocatechin	OH	OH	O
(–)-epicatechin	H	H	OH
(–)-epigallocatechin	OH	H	OH

Figure 2. Example structures of the structurally diverse (**A**) hydrolysable tannins and (**B**) proanthocyanidins. In (**B**), an A-type interflavanoid linkage is highlighted in orange. G = galloyl group, HHDP = hexahydroxydiphenoyl group.

PAs, on the other hand, are oligomers and polymers formed of flavan-3-ol monomeric units, most commonly (epi)catechin and (epi)gallocatechin units. The corresponding PAs formed of these units are referred to as procyanidins (PCs) and prodelphinidins (PDs), respectively. Structural variation is diverse for this group of tannins as well, as the monomeric units can vary by their degree of hydroxylation and the configuration of the C2 and C3, and the positions of carbon-carbon bonds

between the monomeric units can be either C4→C8 (Figure 2B) or C4→C6. PAs can also have an ether linkage between the adjacent monomeric units, called an A-type linkage. This linkage can be formed from the C2 to either O7 (Figure 2B) or O5 of the linked unit. PAs with only carbon-carbon interflavanoid bonds are referred to as B-type PAs, while PAs with one or more additional ether bonds are referred to as A-type PAs. In plants, PAs are present as mixtures of compounds with varying degrees of polymerization, and the isolation of individual higher oligomers has proven difficult.[22–26] Hence, they are commonly described by their mean degree of polymerization (mDP) and by their PC/PD ratio, often referred to as the PC-% or PD-%. PAs can also have other substituents in their structures, e.g., galloyl or glycosyl groups, most commonly attached to the O3 position of the monomeric units (Figure 2B), with other positions also being possible.[27]

The practical benefits of the bioactivities of tannins are of interest, especially in farming, where the rise in anthelmintic resistance (AR) has become a critical issue, affecting both animal health and agribusiness productivity.[28–31] The rapid emergence of AR appears to outpace the development of new anthelmintics, highlighting the need to explore more sustainable strategies for nematode control to effectively address this growing challenge.[32,33] These strategies should include both medical and non-medical approaches, the latter approach including methods such as lowering the infection pressure via rotational grazing and utilizing bioactive forage or feed additives.[34–36] In addition to the antiparasitic properties of tannins, they have been shown to possess other beneficial effects when added to ruminal feed, such as lowering the emission of greenhouse gases and promoting the uptake of nitrogen during rumination.[6,37,38] These beneficial effects are linked to the ability of tannins to form complexes with dietary proteins in the early parts of the gastrointestinal (GI) tract, i.e., rumen, and shield them from degradation during the rumination process.[1,37,39,40] These complexes could then dissociate in the later parts of the GI tract where the chemical environment undergoes major changes, e.g., the shift of pH.[41,42] Ideally, after this condition change, the now-available tannins or their metabolic products could target gastrointestinal nematodes (GINs) and exhibit their anthelmintic activity, lessening the nematode burden for the animals.[43–45]

The antiparasitic and antimicrobial activities of both PAs and HTs have been linked to their protein binding capacities and their affinity to lipids.[12,18] As a consequence, many of the structural features beneficial for protein binding or lipid interactions are important factors in studies on the antiparasitic effects of tannins as well. The overlapping structure-activity patterns are not unexpected, considering that the interactions of tannins are generally described as non-specific, utilizing both hydrogen bonding and hydrophobic interactions.[7,46,47]

Regarding the interactions between PAs and proteins, stronger binding has been observed as a result of the increase in the degree of oligomerization or the molecular

weight, higher degree of hydroxylation (PD-%), and the addition of esterified galloyl groups.[48–51] Also, the presence of additional A-type linkages has been shown to increase interaction with proteins.[52,53] Similarly, studies on lipid affinity conducted with flavan-3-ols and PAs showed increased affinity due to increase in the degree of galloylation or mDP, and the presence of A-type linkages.[54–57] In antiparasitic studies, the greatest antiparasitic effects have been achieved for PAs with high mDP, high PD-%, or for those with additional galloyl groups in their structures.[17,58–60] Equivalent features are also central for the bioactivities of HTs: both the protein binding and lipid interactions are reported to increase as the molecular weight and/or the structural flexibility increase, and by the presence and number of galloyl moieties in the HT structure.[61–65] The antiparasitic activity of purified HTs has been less studied, but comparably to their affinities to proteins and lipids, the increased degree of oligomerization and galloyl moieties have been noted of enhancing the activity.[18,20]

The life cycle of GINs can be divided into three main stages: eggs, larvae, and adults.[66] The larval stage is often divided further into four molts (L1–L4), L3 being the stage where parasitic infection of an animal occurs (Figure 3). During this cycle, the adults residing in the abomasum or the intestines produce eggs, which are then transported through the digestive system and excreted within manure. After hatching, the larval stages L1–L2 develop further in the manure, after which the third stage (L3) larvae move on the forage to be ingested by the host animals. The later development stages occur within the host until the cycle repeats.

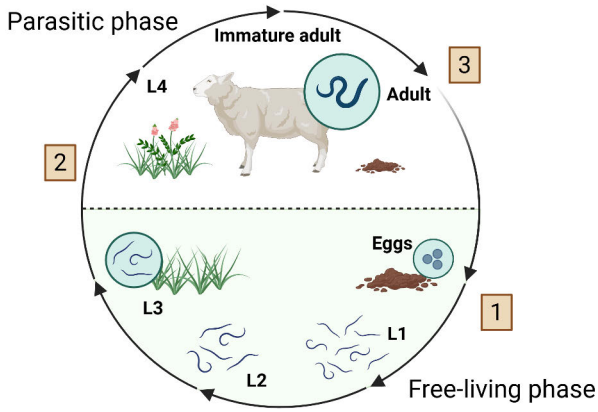

Figure 3. Tannins can restrict nematode development through three approaches along the life cycles of nematodes: (**1**) by inhibiting the egg hatching and development of the first and second-stage larvae (L1 & L2), (**2**) by inhibiting the mobility and exsheathment of the infectious third-stage larvae (L3) and lowering the establishment rate of the larvae, and (**3**) inhibiting the motility of the adult nematodes and reducing egg excretion. Figure adapted with permission from Hoste et al., 2012[36], and created with Biorender.com.

PAs and HTs alike have shown dose-dependent in vitro antiparasitic effects across the life stages of different nematode species, as studied for *Haemonchus contortus* (egg hatching, L1–L4), *Trichostrongylus colubriformis* (L3), *Ostertagia ostertagi* (L1, adults), *Cooperia oncophora* (L1, adults), *Ascaris suum* (L3, L4), and for *Oesophagostomum dentatum* (egg hatching to adults).[17,18,20,58–60,67] In these studies, differences between the inhibition susceptibility of different nematode species were observed, for example, the *T. colubriformis* third-stage larvae were less prone to the effects of tannins than the larvae of *H. contortus*.[17,20,59] These observations could be caused by the differences in the composition of the sheath or the enzymes responsible for the exsheathment process, rather than from any specific interaction mechanisms of tannins.[17] Damage to the exterior of the nematodes exposed to PAs and HTs in vitro and in vivo conditions has been recorded with transmission and scanning electron microscopy (TEM and SEM, respectively).[18,67–70] The main changes observed in these studies were primarily in the cuticle, the buccal area, and the reproductive areas (the third observed only in vitro) of nematodes, likely accounting for the inhibitive effects of tannins on the motility, feeding, and reproduction of GINs (Figure 3).

The in vitro anthelmintic effects of tannins have also been confirmed in vivo with lambs, goats, and cattle by studies utilizing various tannin-rich forage, including sainfoin (*Onobrychis viciifolia*), birdsfoot trefoil (*Lotus corniculatus*), and sericea lespedeza (*Lespedeza cuneata*).[2,70–77] In vivo, tannins have not only exhibited the same actions observed in vitro, such as inhibiting egg hatching, reducing mobility, and affecting exsheathment but have also been observed to reduce the establishment rate of worm populations in the abomasum, likely due to the delayed exsheathment (Figure 3).[76–79] Differences in the inhibition responses of different nematode species have also been observed under in vivo conditions, similar to those seen in vitro.[72,80] However, in some in vivo studies the reported anthelmintic effects of tannins have remained rather low.[81–83] The antiparasitic effects of tannins are highly dose-dependent and linked to specific structural features of tannins, which may play crucial roles in vivo conditions and explain some inconsistencies in results.[38] Additionally, the experimental settings of the studies could have had an impact on the results and in these conditions, the forage itself can contain a variety of compounds in addition to tannins. These compounds could induce unknown cooperative effects and/or provide multiple other potential targets for tannins, lessening the activity against parasitic nematodes.

Since tannins have been proven to affect the entire lifecycle of GINs, their potential could be harnessed through a strategy that combines multiple nematode control methods, rather than relying solely on medication.[84] By doing so, structurally diverse tannins or tannin-rich feeds could be used as complementary nutraceuticals to lower the overall nematode burden and reduce infection pressure in animals.

Additionally, tannins might target nematode strains that exhibit resistance to commercial anthelmintics. These beneficial effects could ultimately contribute to the inhibition of the development of AR.

This complementary approach has been primarily studied with monoterpenes and PA-containing forage, such as sainfoin and redberry juniper (*Juniperus pinchotii*), in combination with common anthelmintics such as albendazole, levamisole, moxidectin, and ivermectin (IVM), through both in vitro and a few in vivo studies.[85–93] However, the results have been inconsistent. Studies showing positive effects from the combination of commercial anthelmintics and natural compounds have reported both synergistic and additive pharmacological effects. These effects stemmed from increased bioavailability of the anthelmintic, increased damage to nematode eggs, and enhanced inhibition of larval motility.[85–90] Conversely, studies reporting negative effects noted reduced pharmacokinetics, leading to lower anthelmintic efficacy which could, in turn, contribute to the development of AR within the surviving helminth populations.[91–93] In all the aforementioned studies, the observed anthelmintic effects of phenolic compounds ranged from no effect[91] to a clear reduction[85,89,90,94] in larval motility and fecal egg count. These variable results emphasize the importance of (poly)phenol structure and concentration, while also highlighting the lack of detailed information on the molecular interactions between natural compounds and (semi)synthetic anthelmintics. In addition, the different nematode strains used in the studies are likely to affect the obtained results as well, as discussed above. This underscores the importance of using well-characterized model tannins in determining bioactivity and highlights the need for more systematic in vivo experiments.

The modes of action of natural compounds behind these inconsistent results mainly remain obscure. One possible mode of action is the direct interaction between natural compounds and commercial anthelmintics. This kind of interaction, or complexation, could either lead to enhanced pharmacokinetics, or it could reduce the bioavailability of the anthelmintic within the animal.[88,91–93] The latter theory has been suggested by Gaudin et al.[93] to at least partially explain their in vivo results of reduced pharmacokinetics, i.e., lower availability of IVM in plasma as a result of a sainfoin-containing diet. Their in vitro studies utilizing PA-rich sainfoin and hazelnut extracts also implicated that both extracts interacted with the anthelmintic dose-dependently and, thus, reduced the available anthelmintic in the rumen fluid. PC-rich hazelnut PAs were observed to be more potent IVM chelators as compared to PD-rich sainfoin PAs.[93]

Another possible mode of action of tannins is their indirect influence on the pharmacological activity of anthelmintics. Tannins may indirectly boost the efficacy of commercial anthelmintics through their protein-binding capabilities, as the damage caused by tannins to the nematode cuticles could potentially enhance the

diffusion of the administered anthelmintic into the target cells.[89] This enhanced concentration in the cells would increase the efficacy of the anthelmintic and as a result, inhibit the development of AR. Other mechanisms could include the affinity of tannins to lipids, as they could interact with the lipid bilayer and cause perturbations, which could in turn potentiate the bioavailability of an anthelmintic.[55] Miro et al.[88] utilized computational approaches in studying the underlying modes of action of monoterpenes on the increased pharmacological efficacy of albendazole observed in vitro. The results indicated that the enhanced anthelmintic efficacy was due to increased membrane permeability as a result of coadministration of monoterpenes and albendazole.[88] Different polyphenols, e.g., flavan-3-ol derivatives, dimeric PAs, and HTs, have been proven to possess affinity to lipids.[11,54,65,95,96] These interactions of polyphenols with lipid membranes consist of polyphenols penetrating the lipid bilayer close to the lipid headgroups, rather than to penetrate through the membrane.[11,97] These interactions could be strong enough to facilitate the diffusion of the administered anthelmintic.

Other indirect activities are also plausible. It is well-established that P-glycoprotein (P-gp) inhibiting drugs have increased the efficacy of anthelmintics, such as macrocyclic lactones (ML), IVM and moxidectin.[87,98–102] In helminths *Haemonchus* spp. and *Cooperia* spp., P-gp has been linked to the development of anthelmintic resistance, as it is the efflux protein responsible for transferring harmful substances to the gut lumen.[102–105] Tannins and other natural compounds have been studied to also possess P-gp modulating abilities, primarily demonstrating inhibitive properties, with some compounds showing an ability to induce P-gp gene expression.[106–108] Quercetin, as a P-gp interfering agent, has been shown to increase the plasma concentration of moxidectin.[87] By increasing plasma concentration and extending the duration of effective levels of the anthelmintic, its pharmacokinetic potential could be enhanced, potentially leading to reduction of the development of resistance.[87] The effect of P-gp modulation on the development of AR and its reversion are further illustrated in Figure 4.

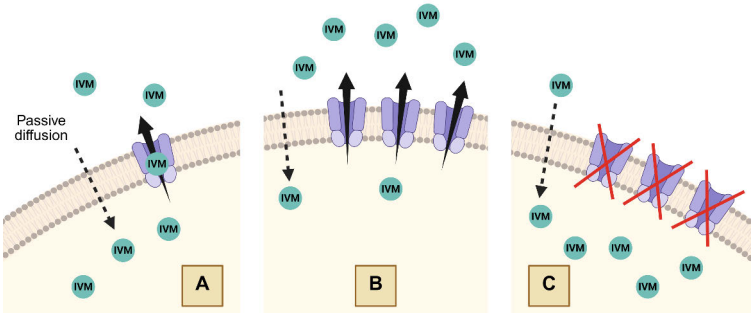

Figure 4. (**A**) Example of normal P-glycoprotein (P-gp) mediated efflux of ivermectin (IVM), (**B**) overexpression of P-gp in response to administered anthelmintic, leading to the development of anthelmintic resistance and (**C**) inhibition of P-gp by a modulating agent and increased concentration of the anthelmintic and toxicity into target cells. Figure adapted from Lespine et al., 2012[101] and created with Biorender.com.

For benzimidazoles (BZs), which is another family of broad-spectrum anthelmintics, similar ways of enhancing the anthelmintic efficacy have been found with drugs modulating the cytochrome P450 (CYP) families.[109,110] These enzymes can function as monooxygenases which oxidize BZs into their less potent and more easily excreted metabolites and, thus, negatively affect the toxicity to the target cells.[111–113] Among natural compounds, flavonoids have been the most studied for their ability to modulate CYP activity, but similar effects have also been observed for other polyphenols as well.[114–118]

Despite their potential, the ability of tannins to reduce the development of anthelmintic resistance via the aforementioned complementary approaches remains largely unharnessed. In vivo studies have shown that tannins can influence the pharmacological efficacy of the commercial anthelmintic IVM, as evidenced by changes in plasma availability and the inhibition of nematode growth or mortality rates.[92–94] These findings suggest that there may be interaction, direct or indirect, between certain tannins and IVM. However, in vivo and in vitro studies have yet to uncover the mechanisms behind these observations, as biological systems are highly complex with a great number of variables. Therefore, simpler models must be used to uncover these mechanisms.

To explore the possibility of direct tannin–anthelmintic interactions, isothermal titration calorimetry (ITC) was employed. ITC was chosen for its ability to detect all kinds of interactions via the quantification of interaction heat and for its sensitivity in measuring the thermodynamics of binding events. Moreover, this method had been previously utilized in the binding studies of tannins to proteins and commercial anthelmintics to proteins.[61,62,64,111,119–124] The basic principle of ITC is the comparison of the temperature difference between two cells - one containing a sample and the other a reference - while maintaining both at equal temperatures. When a ligand is

injected into the sample cell containing the sample, usually a macromolecule, a heat change is induced based on whether the reaction is endothermic or exothermic. The instrument adjusts the temperature of the sample cell to match the reference cell, and this process is repeated through a series of injections, generating a thermogram depicting the power required to regulate the temperature difference. This thermogram can then be analyzed and integrated to produce a binding isotherm, from which key thermodynamic parameters, such as binding affinity (K_a or $1/K_d$), stoichiometry (n), and enthalpy change (ΔH), can be determined via data fitting (Figure 5).

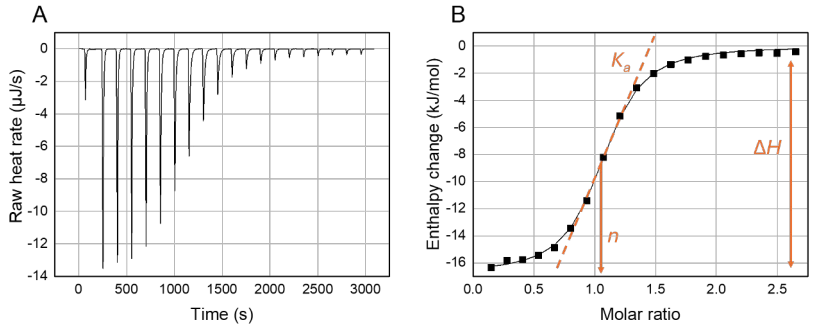

Figure 5. (**A**) Thermogram obtained from isothermal titration calorimetric analysis and (**B**) a binding isotherm derived from the raw data. From (**B**), thermodynamic parameters, such as binding affinity (K_a), reaction stoichiometry (n), and enthalpy change (ΔH) of the interaction can be determined as shown in orange.

However, while ITC is effective in detecting interactions, the interpretation and fitting of thermodynamic data can be complex, and the driving forces behind the interactions may be misinterpreted either due to competing endothermic and exothermic reactions or sub-optimal experiment conditions.[46,125,126] Furthermore, the interaction studies with ITC are often conducted utilizing buffered systems and while these are often suitable for studying biomolecular interactions, the low water solubility of the compounds of interest, such as IVM, can limit the use of ITC. To gain further insights into the mechanisms involved in tannin–anthelmintic interactions, nuclear magnetic resonance (NMR) spectroscopy was also utilized. By the investigation the magnitudes and directions of chemical shifts ($\Delta\delta$s), i.e., the changes in the chemical environment of the tannins and the anthelmintics, through a series of different molar ratios of the polyphenols and anthelmintics, the extent of the interaction between the interacting compounds was assessed and the specific parts of each molecule that were involved in the interaction were identified. The application of NMR spectroscopy also allowed the use of organic solvents, enabling the investigation of compounds with lower water solubility.

In this PhD work, the above-described methodologies were utilized to respond to the following aims:

1. To investigate whether plant tannins interact directly with commercial anthelmintics (**Articles I** and **II**).
2. To study how the structural features of HTs and PAs influence their interaction strength (**Articles I** and **II**).
3. To further investigate the molecular aspects and interaction mechanisms (**Article III**).

To achieve these aims, the project also entailed purification of some of the model HTs used and the production of unique well-defined PA fractions utilizing information[127] and tools[26] previously developed in our research group. The presence of direct interactions between plant tannins and a commercial anthelmintic, thiabendazole (TBZ), was confirmed during the ITC method development process for **Articles I** and **II** and the structural features affecting the strengths of the interaction were studied for HTs (**Article I**) and PAs (**Article II**). The interaction mechanisms of tannins from both tannin classes with model anthelmintics from two different classes, benzimidazoles (TBZ) and macrocyclic lactones (IVM), were studied in more detail by NMR spectroscopy (**Article III**).

2 Materials and Methods

2.1 Extraction, purification, and characterization of model tannins

2.1.1 Sample collection and extraction

HTs used in **Articles I** and **III** were extracted from silverweed (*Argentina anserina*) leaves, willowherb (*Chamaenerion angustifolium*) inflorescence, meadowsweet (*Filipendula ulmaria*) inflorescence, herb bennet (*Geum urbanum*) leaves, purple loosestrife (*Lythrum salicaria*) inflorescence and leaves, raspberry (*Rubus idaeus*) leaves, and black myrobalan (*Terminalia chebula*) leaves. Fresh plant material was collected into 1 l glass bottles which were then filled with acetone. The material was extracted multiple times with acetone/water (4:1, *v/v*). After the extraction of the target compounds, the multiple extracts from the same plant species were combined, the organic solvent was evaporated, and the remaining water phases were lyophilized. Extraction steps were monitored via ultrahigh-performance liquid chromatographic (UHPLC) tandem mass spectrometric (MS/MS) analyses (Section 2.1.3).

Plant materials, i.e., leaves, for the PA fractions used in **Article II** were collected from button fern (*Pellaea rotundifolia*), jungle geranium (*Ixora coccinea*), alpine currant (*Ribes alpinum*), *Heritiera solomonensis*, Japanese plum yew (*Cephalotaxus harringtonia drupacea*), sea grape (*Coccoloba uvifera*), and yew plum pine (*Podocarpus macrophyllus*). After collection, plant material was kept cold to prevent natural enzymes from activating. The plant materials were then lyophilized and ground to fine powder before extraction with a similar protocol as described above. Flavan-3-ols (**Articles II** and **III**) and dimeric PAs (**Article III**) were commercially acquired from ExtraSynthese (Genay, France) with following purities: epicatechin (EC, ≥99%), epicatechin gallate (ECG, ≥97.5%), epigallocatechin (EGC, ≥98%), epigallocatechin gallate (EGCG, ≥98%), PC B2 (≥90%), and PC A2 (≥98%).

2.1.2 Tannin purification by chromatographic methods

For HTs studied in **Articles I** and **III**, the purification protocol consisted of four steps: 1) crude fractionation by Sephadex LH-20 gel in a beaker, 2) fractionation by Sephadex LH-20 gel using column chromatography, 3) preparative fractionation using a high-performance liquid chromatography (HPLC) system coupled to a diode array detector (DAD), and 4) semipreparative purification of target compounds using a similar HPLC system (Figure 6). For the purification of the PA fractions (**Article II**), only steps 2 and 4 were utilized.

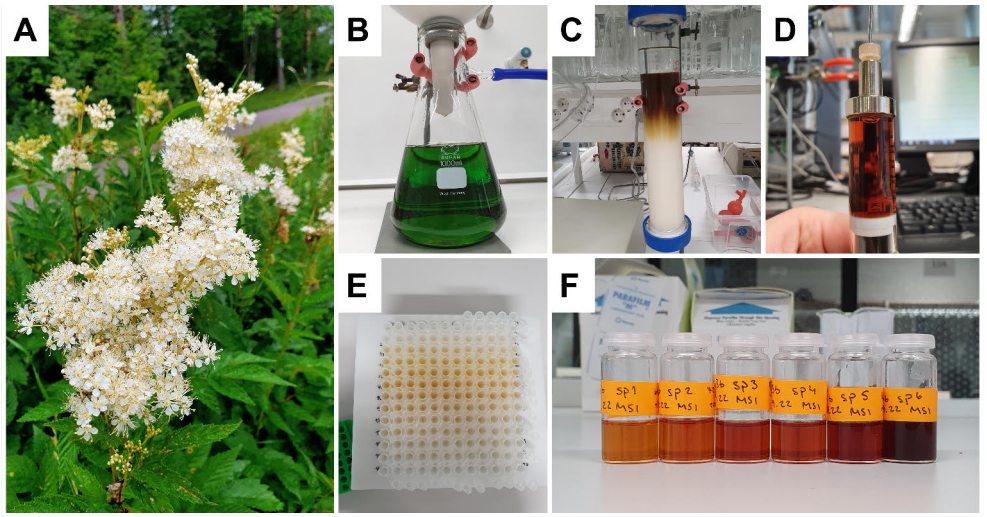

Figure 6. Purification steps utilized in the preparation of model tannins. (**A**) Collection of plant material, (**B**) extraction, (**C**) fractionation with gel chromatography, (**D**) injecting the tannin-rich fraction into high-performance liquid chromatography (HPLC) for preparative and semipreparative fractionation, (**E**) smaller fractions obtained from the purification via HPLC, and (**F**) combined proanthocyanidin fractions.

2.1.2.1 Size exclusion gel chromatography

Crude fractionation of HTs was conducted by first dissolving 50 g of freeze-dried plant extract into type I ultrapure water, filtering the aqueous plant extract using a Büchner funnel with a 125 mm Whatman filter no. 3 (CAT no. 1003-125) and then adding the filtered extract into a large amount of Sephadex LH-20 gel stabilized in ultrapure water. This slurry was stirred for 30–50 min, after which the gel was left to settle on the bottom of the beaker. After most of the gel had settled, the supernatant was filtered through a Büchner funnel, the escaped gel was transferred back to the container, and the procedure was repeated with the next solvent. The solvent profile consisted of water, methanol/water (1:1, *v/v*), methanol, acetone/water (4:1, *v/v*), and acetone, with the number of fractions per solvent modified according to the target compound.

Sephadex LH-20 column chromatography was conducted using a glass column (40 × 4.8 cm i.d., Kimble-Chase Kontes™ Chromaflex™, Vineland, NJ, USA) paired with a peristaltic pump. The Sephadex LH-20 gel was stabilized in water prior to loading the column with the gel. Approximately 5–10 g of the freeze-dried fraction from previous fractionation (HTs, **Articles I** and **III**) or crude plant extract (PAs, **Article II**) was dissolved into 30–50 ml of ultrapure water and filtered through a 0.45 µm polytetrafluoroethylene (PTFE) filter (VWR International, Radnor, PA, USA). Elution profile for HTs was modified from the one previously reported by Salminen and Karonen[128] and consisted of methanol/water (1:1, *v/v*), acetone/water (1:4, *v/v*), acetone/water (3:7, *v/v*), acetone/water (2:3, *v/v*), acetone/water (1:1, *v/v*), acetone/water (3:2, *v/v*), acetone/water (7:3, *v/v*), and acetone/water (4:1, *v/v*). For PAs, the elution profile was similar to the one reported by Leppä et al.[26]; water, methanol/water (3:7, *v/v*), methanol/water (1:1, *v/v*), acetone/water (3:7, *v/v*), acetone/water (1:1, *v/v*), and acetone/water (4:1, *v/v*). The flow rate was 5 ml/min for all Sephadex LH-20 fractionations. After the fractionation, the organic solvent was evaporated and the fractions were lyophilized.

2.1.2.2 Preparative and semipreparative HPLC

Further fractionation of the polyphenol-rich fractions obtained from the Sephadex LH-20 gel chromatography (acetone/water, 4:1, *v/v*) was conducted via an HPLC-DAD system connected to a fraction collector, utilizing a manually filled preparative column (LiChroprep RP-18, 40–60 µm, Merck KGaA, Darmstadt, Germany) and/or a semipreparative column (C-18, Gemini®, 110 Å, AXIA™ Packed, 150 × 21.2 mm, 10 µm, Phenomenex Inc., CA, USA). The eluents were methanol (A1) and aqueous 1% formic acid (B1) for preparative analysis and acetonitrile (A2) and aqueous 0.1% formic acid (B2) for semipreparative analysis.

For the purification of HTs (**Articles I** and **III)**, both preparative and semipreparative methods were used, and the elution profile depended on the target compound, similar to as previously reported.[61] For PAs (**Article II**), only semipreparative fractionation was used with a flow rate of 12 ml/min and the elution profile was as follows: 0–4 min, 8% of A2 in B2; 4–32 min, 8→55% of A2 in B2; 32–33 min, 55→80% of A2 in B2; 35–80 min, 80→8% of A2 in B2 (column wash and stabilization).[26] Sample preparation was conducted by first dissolving 125–150 mg of PA-rich fraction into a small amount of ethanol and diluting this with 2 ml of ultrapure water. The sample was then centrifuged and filtered through a 0.2 µm PTFE filter (VWR International, Radnor, PA, USA). PA fractions were obtained from the unresolved characteristic chromatographic hump and collected into either 2 ml microcentrifuge tubes or 10 ml glass test tubes. These smaller fractions (of either 2 ml or 8 ml) were then combined into six equal sections based on their UV

chromatogram at 280 nm. After fractionation, the organic solvent was evaporated, and the PA fractions were lyophilized.

2.1.3 UHPLC-DAD-MS/MS analyses

The LC-MS instruments used in **Articles I–III** consisted of an Acquity UPLC system (Waters Corporation, Milford, MA, USA) connected to either Xevo TQ triple-quadrupole mass spectrometer (Waters Corp, Milford, MA, USA) or to Q Exactive Orbitrap™ (Thermo Fisher Scientific GmbH, Bremen, Germany). The column used for both instruments was an Acquity UPLC BEH Phenyl column (100 × 2.1 mm, 1.7 µm, Waters Corporation, Wexford, Ireland). The column temperature was 40 °C. LC-MS grade acetonitrile (A) and 0.1% aqueous formic acid (B) were used as eluents.

The elution profile for the characterization of the HTs was as follows: 0–0.5 min, 0.1% of A in B (isocratic gradient); 0.5–5.0 min, 0.1→30% of A in B (linear gradient); 5.0–6.0 min, 30→35% of A in B (linear gradient); and 6.0–9.5 min, column wash and stabilization. (**Articles I** and **III**) The corresponding profile for the characterization of PAs was: 0–0.5 min, 0.1% of A in B (isocratic gradient); 0.5–5.0 min, 0.1→30% of A in B (linear gradient); 5.0–7.0 min, 30→40% of A in B (linear); 7.0–10.2 min, column wash and stabilization. (**Article II)** The injected sample volume was 5 µl. For the analyses, all the samples were dissolved into 10% aqueous ethanol and filtered through 0.2 µm PTFE filters (VWR International, Radnor, PA, USA).

Negative ion mode was used in all MS analyses. The monitoring of the isolation and purification process of HTs (**Articles I** and **III**) was conducted utilizing the TQ mass spectrometer with the electrospray ionization (ESI). The parameters were as follows: capillary voltage 1.8 kV, desolvation temperature 650 °C, source temperature 150 °C, desolvation and cone gas (N_2) flow rates of 1000 and 100 l/h, respectively. The collision gas was argon. The MS analyses of model HTs consisted of a full scan analysis with an *m/z* range of 150–2000 and group-specific multiple reaction monitoring (MRM) methods as previously described.[129] The ESI parameters for the quantitative analyses of PAs (**Article II**) conducted with the TQ mass spectrometer were similar to as described above with the exception of cone gas flow rate of 60 l/h. The MS method consisted of a full scan analysis with an *m/z* range of 150–1200 and group-specific MRM methods as previously described.[129,130] The performance of the instrument during the analysis was monitored via external 1 µg/ml catechin standards. The acquired data was processed with TargetLynx software (MassLynx V4.2 SCN982 © 2017 Waters Corporation, Milford, USA), entailing smoothing (window size 5 scans × 2 smoothing iterations) and integration of the data. To obtain the quantitative data, the integrated PC and PD traces were

processed further utilizing calibration curves made separately for PC, PD, and mDP through thiolysis.[130,131]

For the ultrahigh-resolution MS analysis of the model tannins (**Articles I–III**), the heated ESI parameters for Q Exactive Orbitrap™ were as follows: a spray voltage of 3 kV, a sweep gas flow rate of 0, sheath and auxiliary gas (N_2) flow rates of 60 and 20, respectively, a capillary temperature of 380 °C, the collision gas N_2 and an in-source collision-induced dissociation was applied at 30 eV. The MS method for both tannin classes consisted of full scan and MS/MS analyses. The full scan analyses included an *m/z* range of 150–2250 with a resolution of 35 000 and an automatic gain control of 3×10^6. The MS/MS analyses consisted of a data dependent-MS^2 (TopN) methodology with Top3, stepped normalized collision energies of 20, 50, and 80 eV, a resolution of 17 500, and an automatic gain control of 1×10^5. Pierce ESI Negative Ion Calibration Solution (Thermo Fisher Scientific Inc., Waltham, MA, USA) was used to calibrate the Orbitrap™ prior to analysis. The data was processed with Thermo Xcalibur Qual Browser software (Version 4.1.31.9, Thermo Fisher Scientific Inc., Waltham, MA, USA).

2.2 Isothermal titration calorimetry

MicroCal iTC200 (Malvern Panalytical Ltd., Malvern, UK) was used for all ITC measurements. The state and cleanliness of the instrument were monitored throughout the data acquisition period via water-into-water titrations and an EDTA test kit provided by the manufacturer. The reference cell was filled with type I ultrapure water. A similar sample preparation protocol was used for both HTs and PAs in **Articles I** and **II**, respectively. For the measurements, the concentrations of both the tannins and the anthelmintic (thiabendazole, TBZ) were 3 mM, and a pH 3.6 citrate buffer with either 5% or 10% of dimethyl sulfoxide (DMSO) was used as solvent. Citrate buffer with 10% DMSO was only used if solubility issues were detected with 5% DMSO. The DMSO-% was always the same for the titrant and the analyte to prevent any additional heat due to buffer mismatch. The TBZ solution was prepared by dissolving TBZ into DMSO and diluting this stock solution to the targeted TBZ and DMSO concentrations, while weighed tannins were directly dissolved into the buffer with either 5% or 10% DMSO. For the titrations, the temperature was 40 °C, the injection volume 0.4 µl for the first injection and 2.0 µl for the following 19 injections, the reference power 5 µcal/s, the stirring 750 rpm, the initial delay before the first injection 400 s, and the spacing between injections either 250 s or 200 s for HTs and PAs, respectively. The experiments consisted of one control titration of tannin into buffer and three titrations of tannin into TBZ. Additional control titrations of buffer into buffer and buffer into TBZ were also

conducted, but these resulted in small and equal enthalpy changes and, thus, were not included in the data processing.

The raw data obtained from the instrument was processed with NanoAnalyze software (v. 3.12.0, 2008, TA Instruments, New Castle, DE, USA). During the data processing, the obtained raw thermograms were integrated and the control data of tannin into buffer was subtracted from each of the three replicates of tannin into TBZ. From this, binding isotherms depicting the molar reaction heat per injectant as a function of the molar ratio of tannin to TBZ were obtained and the standard error between replicates was calculated (n = 3). The binding isotherms obtained for rugosin D and B-PC-G 2 were fitted with two independent binding sites model. Data visualization was done using RStudio (version 2024.09.1 Build 394) with "ggplot2" package with assistance from artificial intelligence (ChatGPT, version GPT-4, OpenAI, San Francisco, CA, USA).

2.3 NMR spectroscopy

The NMR experiments in **Article III** were performed utilizing Bruker Avance-III spectrometer operating at 500.12 MHz for ^{1}H and 125.76 MHz for ^{13}C equipped with a Smartprobe (Fälden, Switzerland). The experiment temperature was 298 K, unless otherwise stated. d_3-acetonitrile was used as the solvent due to the limited solubility of the commercial anthelmintics studied. The residual solvent signals were used as references, δ_H = 1.94 ppm and δ_C = 118.26 ppm. TopSpin was used for the operation of the instrument and data analysis (versions 3.6.5 and 3.5 pl 7, respectively, Bruker, Billerica, MA, USA).

For the assignments of polyphenols and the commercial anthelmintics (IVM and TBZ), ^{1}H-NMR and ^{13}C-NMR spectra, along with 2D homonuclear correlation spectroscopy (COSY), rotating-frame Overhauser enhancement spectroscopy (ROESY, with 200 ms mixing time), heteronuclear single quantum coherence (HSQC), heteronuclear multiple bond correlation (HMBC), and selective HMBC spectra (carbonyl region, 166 ± 5 ppm) were recorded. For the interaction studies of selected tannins with TBZ and IVM, only ^{1}H-NMR spectra were collected at 298 K, and the chemical shifts (δ, ppm) were compared to the shifts recorded for pure compounds and shift changes ($\Delta\delta$, $\Delta\delta = \delta_{mixture} - \delta_{pure\ compound}$) were calculated. For the characterization of PC B2, the NMR spectra were recorded at 243 K to prevent the peak broadening due to the hindered rotation around the interflavanoid bond.[132,133] For PC B2, the interaction measurements with IVM and TBZ were recorded at both 298 K and 243 K. Interaction studies were conducted with different molar ratios of polyphenol to anthelmintic with the concentration of tannin always remaining at 0.3 mM. Molar ratios of polyphenol to anthelmintic for studies with IVM were 3:1, 1:1, 1:3, 1:5, and 1:10, and for TBZ 3:1, 1:1, 1:3, and 1:5. Additional

spectra, i.e., ROESY and HMBC, were obtained for mixtures of polyphenols and anthelmintics when necessary for the assignments of the separated OH signals observed in flavan-3-ols and PC A2. Data visualization was done with TopSpin (version and 3.5 pl 7, Bruker, Billerica, MA, USA) and Origin 2016 Sr2 b9.3.2.303 (OriginLab, Northampton, MA, USA).

3 Results and discussion

3.1 Characterization of model tannins

All model tannins were selected to represent different structural features of their representative tannin class. The structures of the model HTs (Figures 7 and 8) contained different numbers of galloyl groups and HHDP groups, an NHTP group, a modified DHHDP group, different degrees of oligomerization and molecular sizes, and different linkages between the monomeric units (*m*-DOG, *m*-GOG, and *m*-GOD). The characterization of the model HTs and their purities are presented in more detail in the supplementary materials of **Articles I** and **III**.

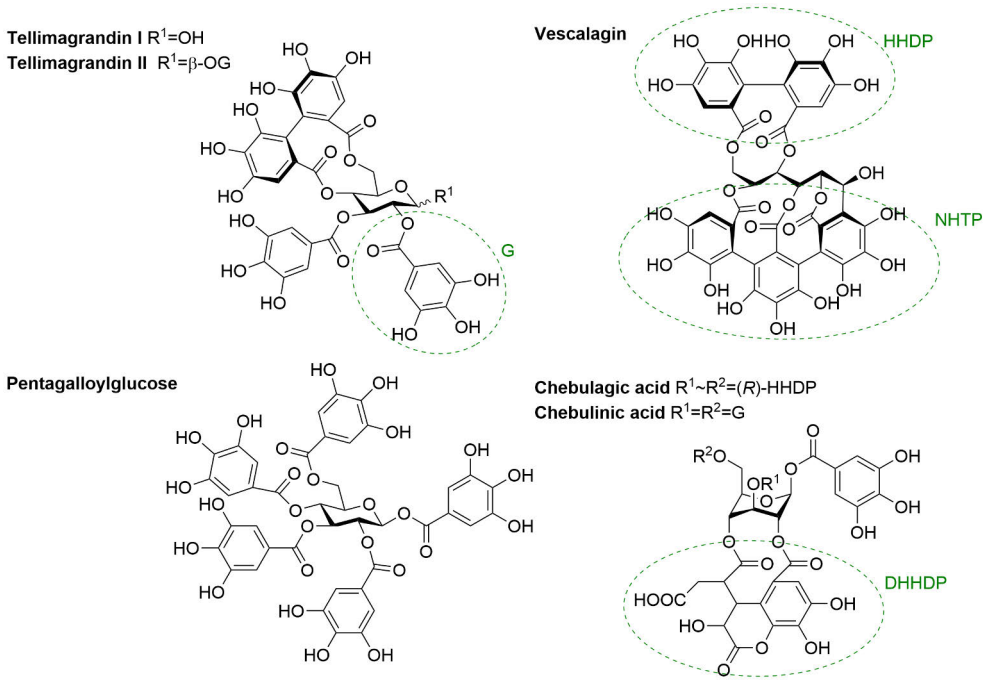

Figure 7. Structures of the hydrolysable tannin monomers studied. DHHDP = dehydrohexahydroxydiphenoyl group, G = galloyl group, HHDP = hexahydroxydiphenoyl group, NHTP = nonahydroxytriphenoyl group.

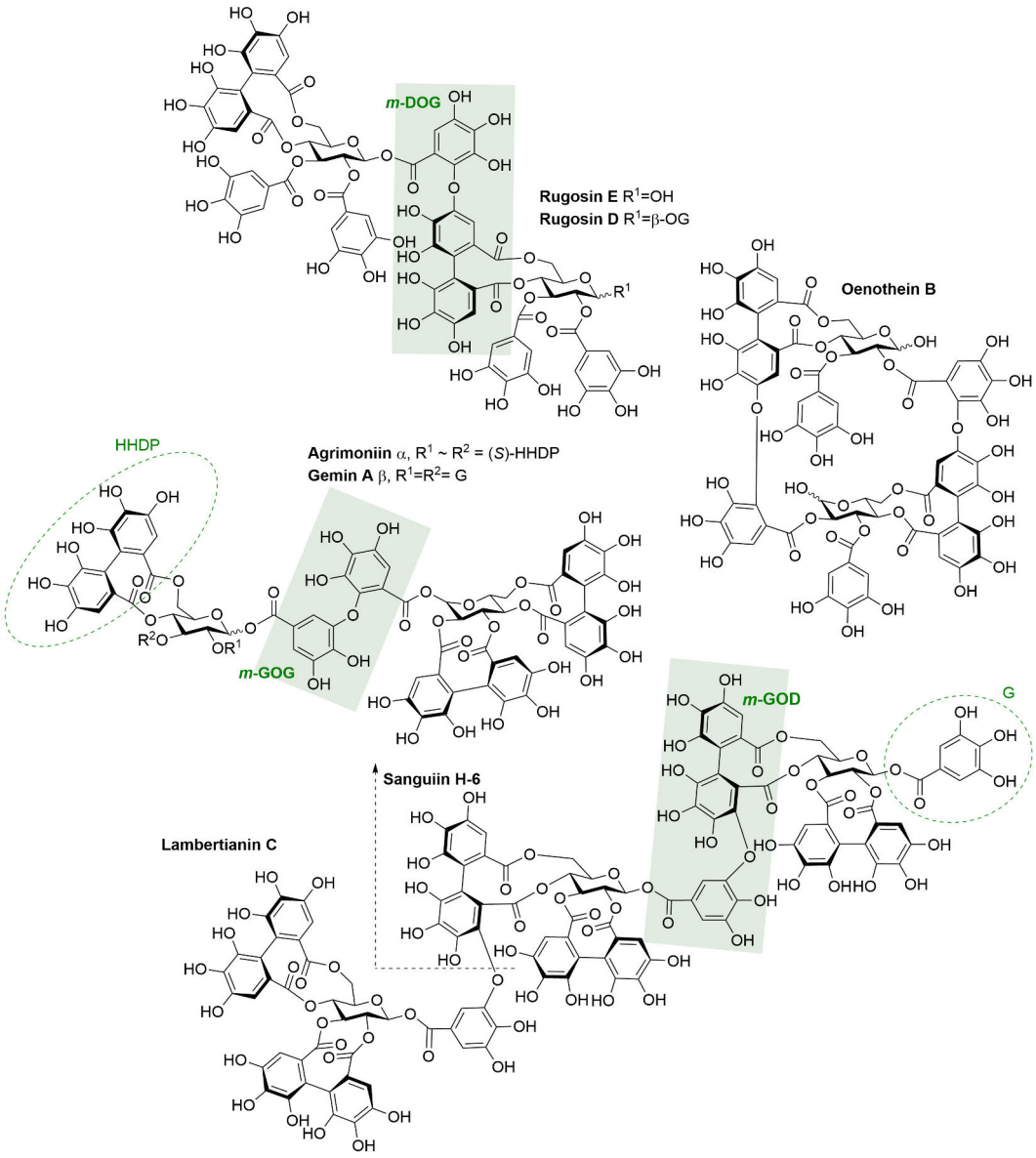

Figure 8. Structures of the hydrolysable tannin dimers and trimer studied. Examples of different types of linkages between monomeric units are highlighted in green: *m*-DOG (valoneoyl group), *m*-GOG (dehydrodigalloyl group), and *m*-GOD (sanguisorboyl group). D = HHDP = hexahydroxydiphenoyl group, G = galloyl group, O = oxygen.

All PA fractions obtained through semipreparative fractionation were characterized both quantitatively using UHPLC-MS/MS with MRM and qualitatively through ultrahigh-resolution UHPLC-MS/MS. (**Article II**) The quantitative approach provided data on the mDP, the PC/PD ratio, and the relative

galloyl content of the PAs, while the qualitative analysis was used to identify interflavanoid A-type bonds and the detailed PA composition. The qualitative results also supported the quantitative estimations. From these fractions, representative ones were selected for the ITC measurements based on the obtained structural characteristics. These fractions, along with their plant origin and structural features, are presented in Table 1. The individual PA compositions obtained through ultrahigh-resolution MS analysis are presented in the supplementary material of **Article II**. A more detailed description of the characterization of PAs can be found in **Article II** and in the references therein.

Table 1. The plant origin and structural features of the proanthocyanidin (PA) fractions used in the isothermal titration calorimetric measurements. The presented number of galloyl groups and the number of A-type linkages are approximations per one PA oligomer or polymer. In the fraction codes, A refers to the presence of A-type bonds and B to B-type PAs. mMW = mean molecular weight, mDP = mean degree of polymerization, PC = procyanidin, and PD = prodelphinidin. Table adapted from **Article II**.

	Sephadex LH-20 fraction[a]			PA profile for each fraction				
Scientific name	mDP	PD-%	Code	mDP	PD-%	Galloyls[b]	#A-type[c]	mMW[d]
Pellaea rotundifolia	11	84%	A-PD 1	11	95%	0.0	1.0	3336.6
			A-PD 2	11	93%	0.0	0.8	3332.6
			A-PD 3	11	70%	0.0	0.5	3323.0
Ixora coccinea	6	1%	A-PC 1	6	1%	0.0	2.0	1727.2
			A-PC 2	10	1%	0.0	3.0	2993.1
			A-PC 3	13	1%	0.0	3.0	3742.7
Ribes alpinum	12	96%	B-PD 1	12	98%	0.0	-	3540.8
			B-PD 2	12	96%	0.0	-	3700.7
			B-PD 3	16	95%	0.0	-	4900.4
			B-PD 4	18	94%	0.0	-	5322.0
Cephalotaxus harringtonia drupacea	6	8%	B-PC 1	6	23%	0.0	-	1810.5
			B-PC 2	7	5%	0.0	-	1879.5
Coccoloba uvifera	6	13%	B-PC-G 1	5	28%	2.1	-	1663.1
			B-PC-G 2	10	12%	3.6	-	3593.1
Podocarpus macrophyllus	10	81%	B-PC/PD	11	69%	0.0	-	3174.8

[a]Proanthocyanidin-rich Sephadex LH-20 fractions prior to semipreparative fractionation. [b]The relative galloyl content calculated from the quantitative data. [c]The approximate number of A-type linkages present in the proanthocyanidin structures. [d]Calculated from quantitative MS/MS data accounting the number of galloyl groups and A-type bonds.

Both of the approaches used were required to fully characterize the obtained PA fractions, as while two fractions might have seemed similar considering the quantitative data only, there could still be large differences in the detailed PA profiles, as revealed by the qualitative ultrahigh-resolution mass spectra. The results in Table 1 reveal the high diversity across the characteristic PA hump, as fractions from the same plant source can greatly differ compared to the original PA-rich Sephadex LH-20 fraction.

From the ultrahigh-resolution mass spectra, the PAs were characterized by exact masses of their main ions, at *m/z* of $n \times 288 + 1$ for PC oligomeric series and at *m/z* of $n \times 304 + 1$ for PD series, and of product ions produced by their characteristic fragmentation patterns: heterocyclic ring fission (HRF), retro-Diels-Alder (RDA) fragmentation, and quinone-methide (QM) cleavage (Figure 9).[132,134–138] For example, QM cleavage of a PC dimer yields ions at *m/z* 287 and 289 from the extension and terminal units, correspondingly (Figure 9). In the mass spectra presented in **Article II**, it can be observed that the ion at *m/z* 289 is in abundance compared to the ion at *m/z* 287, and thus, it is likely that direct cleavage of the interflavanoid bonds occurs as well (Figure 9). All the PA fractions studied in **Article II** were not pure PCs or PDs, but rather PC/PD mixtures. PA oligomers consisting of both PC and PD units appeared as clusters of similar ions with 16 Da difference around the ions calculated for the corresponding oligomers of only PC or PD units. With the use of ESI, higher PA oligomers can form multiply charged ions. For example, a PA series starting from heptamers can appear as doubly charged ions at *m/z* $1008 + n \times 144$ for PCs or at *m/z* $1064 + n \times 152$ for PDs. The abundances of these ions are typically lower than for those of smaller oligomers, as the efficiency of ionization decreases with the increase of the degree of polymerization of the PAs.[139] Ions with smaller *m/*z detected in the mass spectra can also be fragments of these higher oligomers.

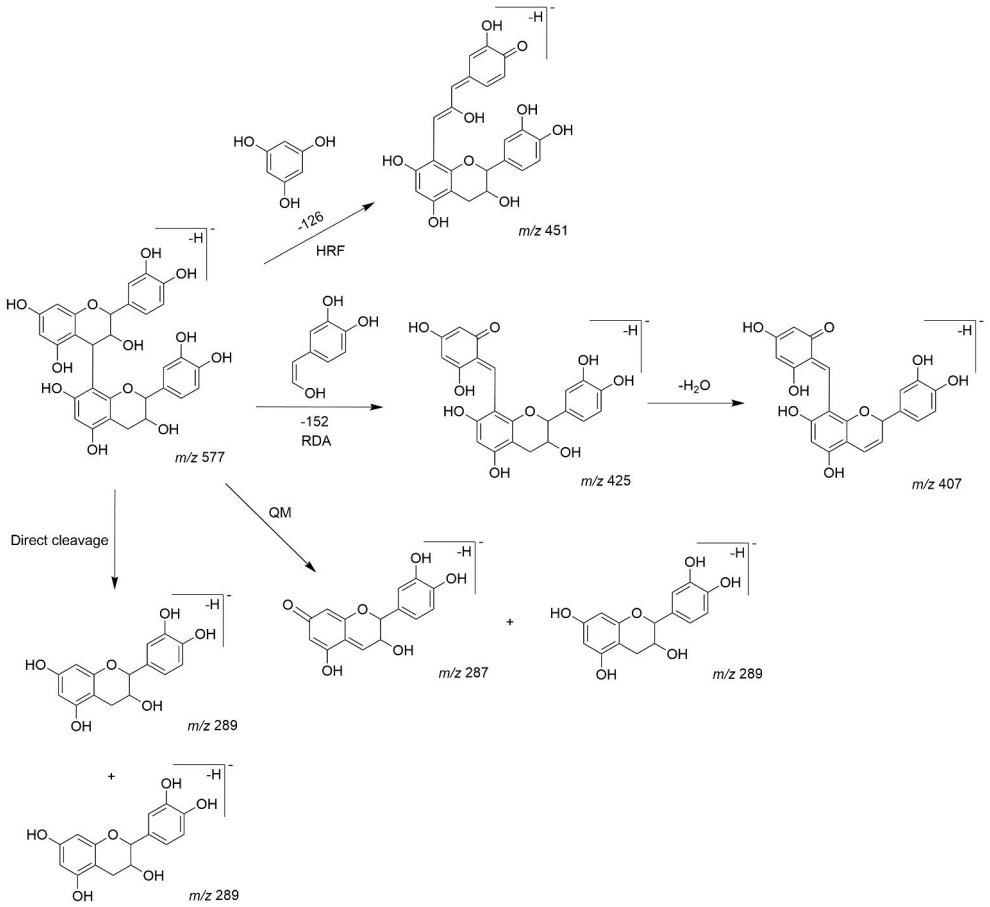

Figure 9. Characteristic fragmentation pattern of a B-type procyanidin dimer. The mechanisms are heterocyclic ring fission (HRF), retro-Diels-Alder (RDA) fragmentation and the sequential loss of water, quinone-methide (QM) cleavage, and direct cleavage.[132,134–138]

Some of the obtained fractions also contained PAs with A-type bonds and additional galloyl groups. From the ultrahigh-resolution MS data in **Article II**, we could observe the presence and the number of the A-type bonds, as an oligomer containing an A-type interflavanoid linkage appears in the mass spectrum as a strong signal with a mass difference of 2 Da when compared to the corresponding B-type PA. While the mass difference of 2 Da can be easily observed, careful identification is required in the determination of the authenticity of an alleged A-type bond, as similar ions can also originate from oxidation or fragmentation of a B-type PA. This can be achieved by examining the retention time of the PA, the product ion spectrum, and the characteristic fragmentation patterns of PAs.[137,138,140,141] However, generally MS data cannot reveal the precise locations of these bonds in the PA structure. Galloylated PAs could be detected by the presence of a fragmentation at *m/z* of 169,

corresponding to gallic acid, and/or by the addition of 152 Da to the observed *m/z* of the corresponding nongalloylated PA. If an oligomer is suspected of containing multiple galloyl groups, the accurate masses of the corresponding ions from ultrahigh-resolution mass spectra should be compared to the calculated accurate masses, as at the integer level, the mass of two galloyls (2 × 152 Da) corresponds to that of an additional PD unit (304 Da).

3.2 Thermodynamic binding studies

A systematic study of the structural properties of HTs, flavan-3-ols, and PAs affecting the interaction with a commercial anthelmintic, TBZ (Figure 10), was inspected via ITC (**Articles I** and **II**). The method development for the comparison of different polyphenols required testing of different solvents, concentrations, and equipment parameters in order to obtain data that could produce binding isotherms from which thermodynamic parameters of the interaction could be obtained. As the interaction profiles ranged from almost no interaction to strong interactions, compromises for the experimental method had to be made in order to achieve a sigmoidal thermodynamic interaction profile for some of the interacting components while also being able to systematically compare all studied compounds with each other. The developed method was applicable for this purpose and was successfully used in **Articles I** and **II** to obtain comparable interaction data for different polyphenols.

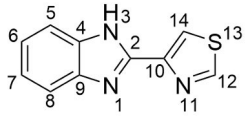

Figure 10. The model anthelmintic, thiabendazole (TBZ), used in the isothermal titration calorimetric analyses.

While the method used did not produce sigmoidal binding isotherms for all samples, the obtained enthalpy changes, revealing the strengths of the interactions, could be compared to the structural features of the polyphenols. The obtained enthalpy changes for the interactions of polyphenols and TBZ ranged from 0 kJ/mol to larger exothermic ones of approximately –30 kJ/mol, with the interactions between PAs (with larger molecular weights) and TBZ generally resulting in larger enthalpy changes than observed for HT-TBZ interactions (Figure 11). Overall, these interaction strengths were weaker in comparison to, e.g., interactions of tannins with proteins.[61,62,142] However, the interaction strengths could be measured and responded to our first aim; we witnessed direct interactions between plant tannins and TBZ.

Individual binding isotherms for all the samples analyzed can be found in their respective articles (**Article I** for HTs and **Article II** for flavan-3-ols and PAs).

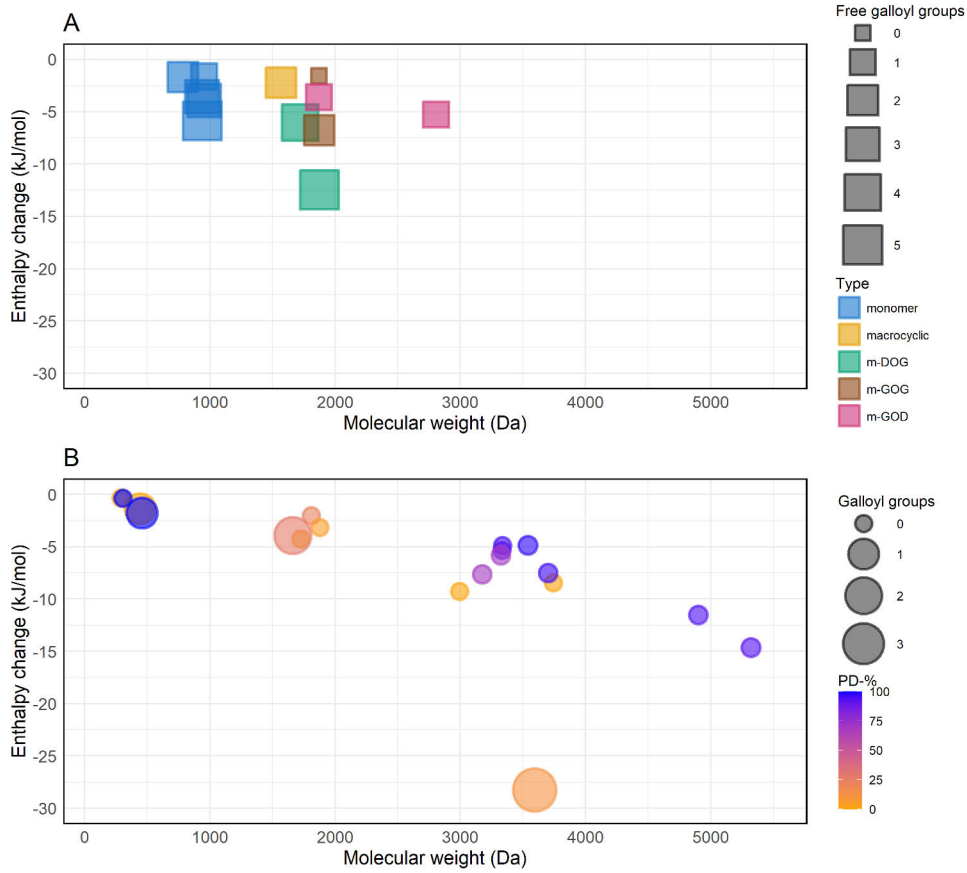

Figure 11. Results from the isothermal titration calorimetric binding studies for the interaction of (**A**) hydrolysable tannins (HTs) and (**B**) proanthocyanidins (PAs) with thiabendazole, presented as the observed enthalpy change of the first real injection of the titration series as a function of molecular weight. The presence of galloyl groups is indicated by the size of the data points for both graphs and the color of the data points is dictated by either the linkage type between monomeric units (HTs, graph A) or the prodelphinidin-% (PD-%, PAs, graph B). *m*-DOG = valoneoyl group, *m*-GOG = dehydrodigalloyl group, and *m*-GOD = sanguisorboyl group.

Overall, the strength of the interaction correlated with the increasing molecular weight, but the other structural characteristics, i.e., different functional groups, determined the final interaction strength (Figure 11). The most important structural feature in increasing the interaction strength was the presence of galloyl groups in the polyphenol structure, as noted for all polyphenols studied (Figure 11). For HTs,

for example, rugosin D, a dimer with five free galloyl groups in its structure, exhibited the largest observed enthalpy change (–13 kJ/mol) while lambertianin C, a trimer with only one galloyl group, produced an enthalpy change of only –5 kJ/mol. (**Article I**) Also, HT monomers with free galloyl groups exhibited larger enthalpy changes than agrimoniin, a HT dimer with no galloyl groups (Figure 11, **Article I**). For PAs, a similar observation was made as the galloylated PAs (mDP of 10, fraction B-PC-G 2, Table 1) produced an enthalpy change of –28 kJ/mol while the enthalpy change was –15 kJ/mol for a non-galloylated PA fraction with a higher mDP (mDP of 18, fraction B-PD 4, Table 1, **Article II**). Higher mDP was still an important factor even with the presence of galloyl groups, as indicated by the enthalpy change of –4 kJ/mol for galloylated PC fraction (mDP of 5, fraction B-PC-G 1, Table 1, **Article II**) compared to the change of –9 kJ/mol for higher non-galloylated PC fraction (mDP of 10, fraction A-PC 2, Table 1, **Article II**).

For HTs, the effect of the molecular flexibility was important for their interaction with TBZ, as proved by small enthalpy changes acquired for vescalagin (0 kJ/mol, **Article I**) with an acyclic polyol core and a rigid NHTP group, and for a macrocyclic ET dimer, oenothein B (–2 kJ/mol, **Article I**). A similar effect was observed when the degree of molecular flexibility and the number of free galloyl groups decreased with the formation of HHDP groups, as the enthalpy changes for HT monomer-TBZ interactions were: pentagalloylglucose > chebulinic acid ≈ tellimagrandin II > tellimagrandin I ≈ chebulagic acid > vescalagin, with the largest enthalpy change representing the strongest interaction. Also, the molecular flexibility of the HT dimers and the trimer is affected by the linkage type between the monomeric units. Here, the linkage types *m*-DOG, *m*-GOG, and *m*-GOD were represented, with oenothein B having two *m*-DOG linkages, forming a macrocyclic structure (Figure 8). Of these, the macrocyclic structure is the most rigid, followed by DOG and GOD linkages, while GOG linkage results in the greatest flexibility. The effect of the linkage type can be seen in Figure 11A, as even though the number of galloyl groups took precedence, the most rigid structure (oenothein B) exhibited smallest enthalpy change of the dimers, and as a dimer with two galloyl groups and *m*-GOG linkage (gemin A, **Article I**) exhibited a similar enthalpy change compared to a dimer with four free galloyls and a *m*-GOD linkage (rugosin E, **Article I**).

For the PAs, the additional A-type linkages inducing rigidity had little effect on the interaction strength. The differences noted between A- and B-type PA fractions could be attributable to the effect of mDP, as the oligomeric distribution of individual PAs observed in the ultrahigh-resolution mass spectra was different for the compared A-type and B-type fractions. (**Article II**) Our results suggested that a lower degree of hydroxylation (PC-rich PAs) would lead to larger observed enthalpy changes in comparison to higher degree of hydroxylation (PD-rich PAs, Figure 11B), but according to the ultrahigh-resolution mass spectra obtained for the fractions (**Article II**), the mDP

was also slightly higher for these PC-rich fractions, which might have accounted for the observed results as well. Also, no significant differences in enthalpy changes were observed for the interactions between TBZ and flavan-3-ol monomers, epicatechin and epigallocatechin. Therefore, it could be concluded that the hydroxylation degree did not significantly influence the interaction between PAs and TBZ.

While most of the data produced non-sigmoidal binding isotherms which could not be reliably fitted without the knowledge of the stoichiometry of the reaction[126,143,144], we could fit the data of one binding isotherm from both tannin class, rugosin D (HTs) and fraction B-PC-G 2 (PAs), and determine the thermodynamic parameters of the interactions (Figure 12, Table 2). Certain characteristics of these two samples are similar, as they both have relatively high molecular weights compared to the rest of the compounds studied (Figures 7 and 8, Table 1) and have several free galloyl groups in their structures. These characteristics, as discussed above, are likely the reason why these tannins exhibited interactions strong enough for the binding isotherms to be reliably fitted. In Figure 12B, the observed exothermic response increased during the first injections of B-PC-G 2 to TBZ, indicating cooperative binding taking place from the addition of tannin into the sample cell[119,122,145]. Therefore, the first two data points were not included in the fitting process of B-PC-G 2.

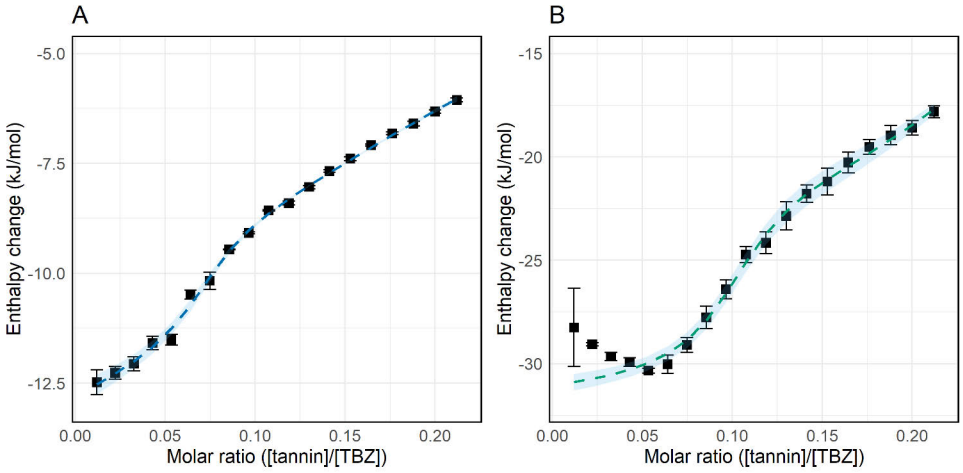

Figure 12. Binding isotherms (■) and data fits with a model of two individual independent binding sites (dashed line) for the interactions of (**A**) rugosin D and (**B**) fraction B-PC-G 2 with thiabendazole (TBZ). The standard error between fits is presented by a blue shade (*n* = 3). The first two data points in (**B**) were not included in the fitting process.

The thermodynamic parameters of rugosin D and B-PC-G 2 obtained from the fitting of the binding isotherms had similar characteristics: the affinity constants (K_{a1}

and K_{a2}) were on almost similar levels, the small reaction stoichiometries (n_1 and n_2) revealed that the smaller molecule, TBZ, acts as a ligand in these reaction and binds more to the tannin during the first part of the interaction (depicted by n_1), and observed enthalpy change (ΔH) was smaller in the first part of the interaction (ΔH_1). The K_{a1} and K_{a2} values of the interaction between rugosin D and TBZ (K_{a1} of 1.5 × 10^5 M^{-1} and K_{a2} of 3.8 × 10^3 M^{-1}, Table 2) were quite typical for ITC data, as they correspond to the first binding site of being tighter, followed by a less tight secondary site, similarly to the binding of HTs to proteins.[61,62] In the case of the PA fraction, however, the binding affinities K_{a1} and K_{a2} were more similar (1.0 × 10^5 M^{-1} and 3.2 × 10^4 M^{-1}, respectively, Table 2), indicating that both of the binding instances taking place were of more similar strengths. Interestingly, despite the size differences of the molecules, the stoichiometries of the interactions for both tannins were the same (Table 2). However, it is important to note that the PA fraction is a mixture of multiple different PAs with molecular weights ranging from hundreds to thousands of daltons, and that the stoichiomerty obtained for this interaction represents an average value. Notably, the secondary binding sites of both interactions were more exothermic than the first binding sites, which was unexpected since tighter interactions typically produce more exothermic responses.

Table 2. Thermodynamic parameters were obtained for the interactions of rugosin D and B-PC-G 2 fraction to thiabendazole using a model with two independent binding sites. K_{a1} and K_{a2} are the affinity constants for the two sets of binding sites, n_1 and n_2 represent the reaction stoichiometries, and ΔH_1 and ΔH_2 represent the corresponding enthalpy changes. ΔG is the free Gibbs energy of the binding and ΔS the entropy change.

	Thermodynamic parameter	Rugosin D	B-PC-G 2
Binding site 1	K_{a1} (M^{-1})	(1.5 ± 0.4) × 10^5	(1.0 ± 0.1) × 10^5
	n_1	0.1 ± 0.0	0.1 ± 0.0
	ΔH_1 (kJ/mol)	-2 ± 0	−9 ± 1
	ΔG_1 (kJ/mol)	-31 ± 1	-31 ± 1
	ΔS_1 (kJ/mol)	92 ± 2	72 ± 6
Binding site 2	K_{a2} (M^{-1})	(3.8 ± 1.2) × 10^3	(3.2 ± 0.6) × 10^4
	n_2	0.3 ± 0.0	0.3 ± 0.0
	ΔH_2 (kJ/mol)	-15 ± 2	−23 ± 1
	ΔG_2 (kJ/mol)	-21 ± 1	-27 ± 1
	ΔS_2 (kJ/mol)	21 ± 8	9 ± 9

From the binding constant K_a (Table 2), the free Gibbs energy (ΔG) could be determined:

$$\Delta G = -RTlnK, \quad (1)$$

where R is the universal gas constant and T is the absolute temperature in Kelvin. Entropy (ΔS) could be calculated from the second law of thermodynamics:

$$\Delta G = \Delta H - T\Delta S \quad (2)$$

The obtained Gibbs free energy (ΔG) and entropy (ΔS) values for the rugosin D and the PA fraction were quite similar in the first binding site, with B-PC-G 2 fraction exhibiting slightly smaller ΔS (Table 2). Small differences were also found in the secondary binding sites, as the PA fraction exhibited slightly smaller ΔG and ΔS values. The values for both tannins and both binding sites indicated that the observed reactions were spontaneous ($\Delta G < 0$) and entropically driven ($\Delta S > 0$), suggesting that hydrophobic interactions were the main driving forces in these interactions.[125,142] These findings are consistent with our qualitative results, as the most significant factor was the presence and number of free galloyl groups. These groups can interact through hydrophobic interactions such as π–π stacking, though also through hydrogen bonding, due to their phenolic structures. However, as the observed ΔH can be a sum of competing endothermic and exothermic reactions and is affected by experimental conditions, the obtained ΔS should be treated with caution.[46,125] Thus, the presence of hydrogen bonding in these interactions should not be ruled out. This could be especially relevant in the case of the smaller ΔS_1 and ΔS_2 of the B-PC-G 2 fraction compared to the values obtained for rugosin D, as the PA fraction has more plausible binding sites for hydrogen bonding.

3.3 Interaction studies by NMR spectroscopy

To complement the information on structure–activity relationships gained from ITC, NMR spectroscopy was utilized to delve deeper into the interaction mechanisms of polyphenols and anthelmintics (**Article III**). Moreover, the use of deuterated acetonitrile with NMR spectroscopy allowed the inclusion of another commercial anthelmintic into the study, widely used IVM from the family of macrocyclic lactones. Thus, the interaction mechanisms of examples from two different anthelmintic families could be compared. The included polyphenols for the NMR analysis were flavan-3-ols EC, ECG, EGC, EGCG, two PC dimers PC A2 and PC B2, and HTs tellimagrandin I, tellimagrandin II, vescalagin, PGG, and gemin A. Commercially acquired PA dimers were used instead of the PA fractions used in ITC study for more accurate ^{1}H-NMR characterization of the signals of the dimers. This

approach allowed, e.g., the comparison of the interaction susceptibilities of the extension and terminal units of the PA dimers (**Article III**).

The interpretation of NMR data included qualitative comparison of the ^{1}H-NMR spectra of the polyphenol-anthelmintic mixtures to those recorded for the pure compounds and quantitative analysis, where the chemical shifts (δ) of the signals present in the mixtures were compared to those of the pure compounds, allowing the calculation of the chemical shift changes ($\Delta\delta$, $\Delta\delta = \delta_{\text{mixture}} - \delta_{\text{pure compound}}$). These $\Delta\delta$s provided insights into the interaction mechanisms of the studied interactions, as the chemical environments of investigated nuclei change due to the proximity of the other interacting component.[11,97,146–149] These changes were not present for all signals observed, indicating that the perceived $\Delta\delta$s were not only caused by the addition of the other component into the solutions but were an indication of interaction. Qualitative differences in the proton signals between the polyphenol-anthelmintic mixtures and pure compounds were also observed, with differences noted for the signals of TBZ with the mixtures of all studied polyphenols and for IVM only in the mixtures with HTs (**Article III**). The qualitative changes for the signals of TBZ were the sharpening of the signals for H-6 and H-7 and the coalescence of H-5 and H-8 (Figure 10), indicating the disturbance of intramolecular hydrogen bonding by the introduction of the interacting component, i.e., the polyphenol. For IVM, the corresponding qualitative changes were the broadening of the OH signals in the spectrum (**Article III**). These types of clear indications of interaction were also observed for the proton signals of the polyphenols, as the broad OH signals of the flavan-3-ols and PC A2 separated and sharpened with the addition of the anthelmintics (Figure 13). These separated signals could be assigned from the mixtures, allowing further investigation of the binding affinity of the different parts of the compounds. Similar effect was not seen with the OH signals of the HTs studied.

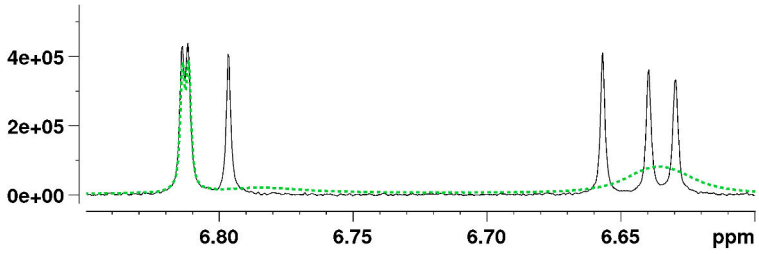

Figure 13. The sharpening of the broad hydroxyl group signals of epicatechin (EC), shown in green dashed line, with the addition of the anthelmintic. The mixture of EC and thiabendazole at a molar ratio of 1:1 is shown in black line.

The observed Δδs within the molar ratio series not only revealed the interaction affinity through the comparison of the magnitudes of the chemical shifts but also provided information on the interaction mechanism through the direction of the shifts (upfield or downfield). Additionally, they indicated the orientation of TBZ relative to the interacting component via ring-current effects.[150,151] Upfield Δδs within the molar ratio series, strongly present in the interactions with TBZ, are likely to be induced by the shielding ring-current effects when the proton is located above the aromatic ring such as in π-π stacking. (**Article III**) In these instances, protons exhibiting downfield shifts are subjected to the deshielding effect and located at sides of the ring, perpendicularly to the aromatic plane.[150] Deshielding effects can also be caused by other types of interaction, e.g., hydrogen bonding.[152] For instance, downfield Δδs within the molar ratio series were observed for the hydroxyl groups of flavan-3-ols and dimeric PAs and linked to hydrogen bonding. (**Article III**) Similarly, downfield shifts within molar ratio series were also observed for the OHs of IVM, but these could also be caused by the changes in the molar proportion of IVM throughout the molar ratios. However, the Δδs of the OHs of IVM were similar between the flavan-3-ols and PA dimers but varied with the HTs, implying that the Δδs observed were induced by the interaction rather than the changing molar proportion. (**Article III**)

Differences in the interaction affinities between the studied anthelmintics could be observed in all polyphenol-anthelmintic mixtures. (**Article III**) For example, in the mixtures of gemin A and IVM, the Δδs within the molar ratio series were minor, whereas distinct changes were observed in the mixtures with TBZ (Figure 14). In the mixtures with TBZ, the orientation of the interacting components was indicated through the upfield and downfield Δδs observed as the molar proportion of TBZ increased (Figure 15).[150,151] This was observed also for other tannins but was especially distinguishable in the interactions between gemin A and TBZ (Figures 14B and 15). With the increase of the molar proportion of TBZ, the proton signals of gemin A generally shifted upfield, except for H-1b, H_A-3, and H_G-3, for which downfield shifts were observed (Figures 14B and 15). The direction of the Δδs of H_F-3 were upfield, and this would indicate the orientation of the aromatic rings of TBZ of being parallel to the ring plane of the F galloyl moiety of gemin A (Figure 14).[151,153] Consequently, the surrounding protons could experience the deshielding effects of the ring-current, as shown for H-1b, H_A-3, and H_G-3. The downfield shifts experienced by H_G-3 could also stem from hydrophobic interactions of the other HHDP or galloyl moieties, such as H_H-3.

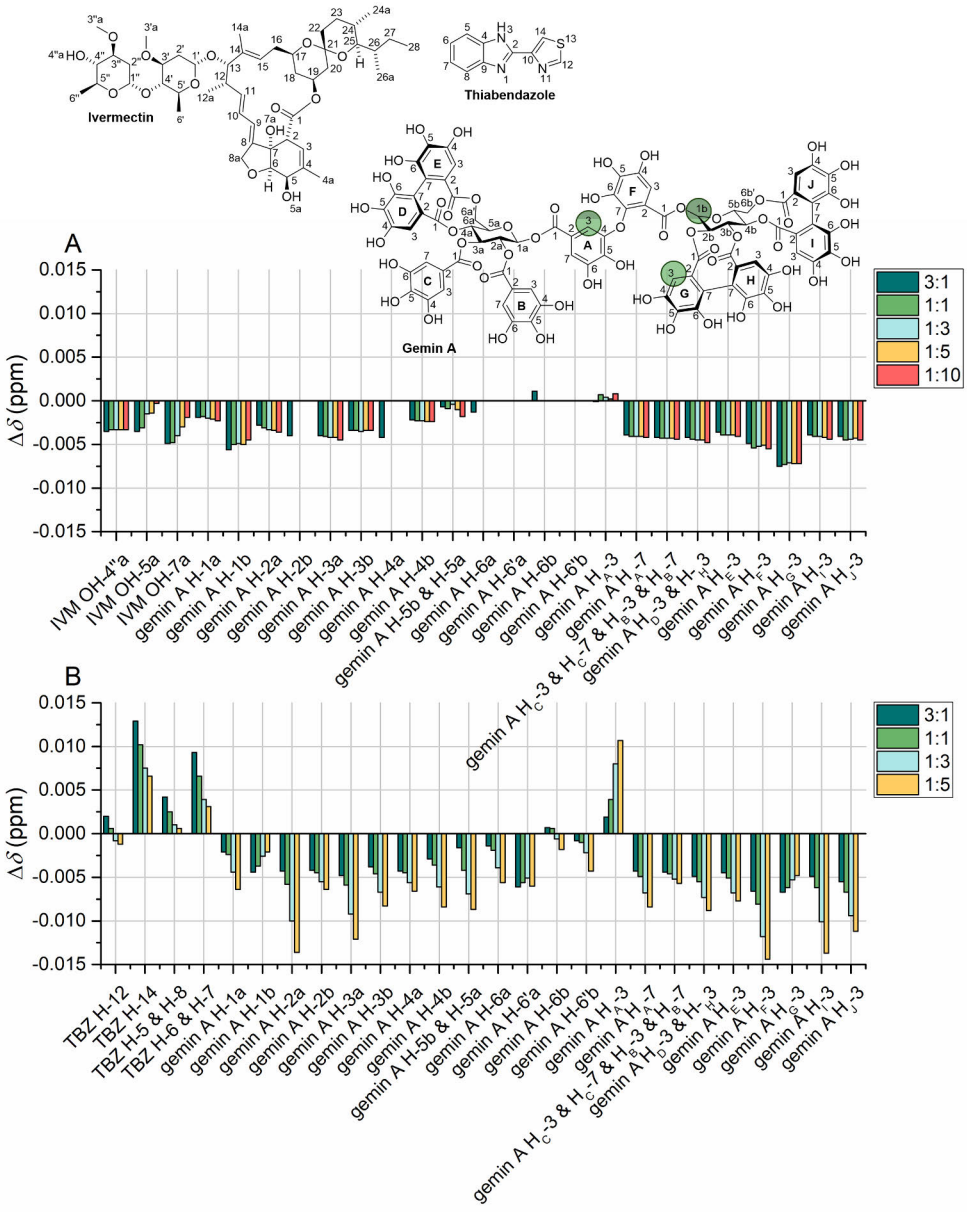

Figure 14. ^{1}H-NMR chemical shift changes (Δδs, $\Delta\delta = \delta_{mixture} - \delta_{pure\ compound}$) observed in the mixtures of gemin A and (**A**) ivermectin (IVM) and (**B**) thiabendazole (TBZ) at different molar ratios of gemin A to the anthelmintic. Proton signals of gemin A showing downfield Δδs with the increased molar proportion of TBZ, H_A-3, H-1b, and H_G-3, are highlighted. Δδs are shown for the signals of the anthelmintics for which Δδs or qualitative changes could be observed and for all signals of gemin A. Missing data is due to overlapping signals of the components or as no Δδs were observed. Figure adapted from **Article III**.

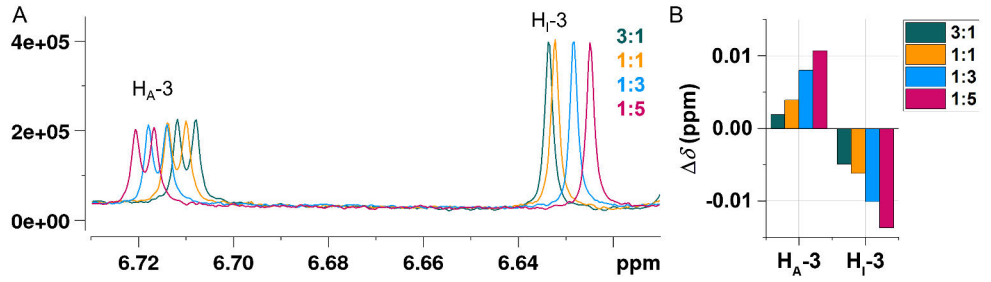

Figure 15. (**A**) Downfield chemical shift changes ($\Delta\delta$, $\Delta\delta = \delta_{mixture} - \delta_{pure\ compound}$) were observed for the proton signal H_A-3 of gemin A and upfield changes for the signal of H_I-3 with the increasing proportion of thiabendazole (TBZ) in the molar ratio series of gemin A to TBZ. (**B**) $\Delta\delta$s for H_A-3 and H_I-3 at different molar ratios of gemin A to TBZ.

Differences in the interaction mechanisms were also observed depending on the polyphenol class, though all studied polyphenols exhibited larger $\Delta\delta$s in the mixtures with TBZ than with IVM, as also exemplified in Figure 14. (**Article III**) With flavan-3-ols and PAs, the interaction sites with both anthelmintics were more focused on the OHs in the structures of the polyphenols, with larger $\Delta\delta$s observed for aromatic than aliphatic OHs. With HTs, however, the observed $\Delta\delta$s were more evenly distributed throughout the aliphatic and aromatic protons of the tannin, especially in the mixtures with TBZ. This would indicate that flavan-3-ols and PAs relied more on the formation of hydrogen bonds in their interactions and for HTs, the interaction mechanisms were more focused on hydrophobic interactions. In HT–TBZ interactions, π-π stacking or other hydrophobic interactions of TBZ with the different galloyl moieties of HTs, i.e., both galloyl and HHDP groups, could exert their influence onto the aliphatic protons of the glucose core, causing the more distributed $\Delta\delta$s.[47] These highlighted structural features aligned quite well with the results obtained by ITC, although the larger magnitudes of $\Delta\delta$s of the OHs of flavan-3-ols compared to the $\Delta\delta$s of the aliphatic and aromatic protons HTs show different trend than seen with the enthalpy changes obtained by ITC (**Articles I–III**). However, these differences could be attributed to the differences in the molar ratios and solvents between the studies and to the observation that for HTs, the $\Delta\delta$s are more evenly distributed throughout the molecule while with flavan-3-ols, the $\Delta\delta$s are almost solely present in the OHs. This kind of difference could lead to the interaction of more TBZ with HTs, leading to larger observed enthalpy changes in the ITC data.

4 Conclusions

This work was driven by the need to better understand tannin–anthelmintic interactions due to reports of both enhancement and inhibition of the anthelmintic efficacy of oral drenches by tannins in vivo. Similar indications of both synergism and antagonism between the two have also been observed in vitro. As these contradictory results were obtained from studies incorporating complex biological systems, this work utilized simplistic settings with only two components, the selected tannin and the anthelmintic, to identify the related structure-activity patterns between these two.

ITC analyses proved that the interactions between plant tannins and commercial anthelmintics exist and are mediated by the structural characteristics of tannins. For both HTs and PAs, the strongest interaction originated from the presence and number of free galloyl groups combined with higher molecular weight. NMR spectroscopy proved to be an insightful tool to complement the ITC data. The results from NMR investigations showed distinct differences in interacting components between two anthelmintic classes, benzimidazoles and macrocyclic lactones, highlighting the necessity of understanding the chemical reactions at play when combining two, or multiple, anthelmintics. The results also showed that the prominent interaction mechanism for IVM could be the formation of hydrogen bonds while with TBZ, the interactions with polyphenols could be driven by both hydrogen bonding and hydrophobic interactions. The involvement of these mechanisms aligned well with the findings with ITC.

The structural features affecting the interactions of tannins and anthelmintics were mostly in line with those observed for the other bioactivities of tannins, most notably protein binding capacity and affinity to lipids. These structural features are also highly represented in the antiparasitic studies of tannins, and they have also been suspected of facilitating the access of commercial anthelmintics to their target sites via the means of membrane perturbation and cuticle impairment. Possibly, the most beneficial combination of tannins and commercial anthelmintics to animal welfare might be one where tannins exhibit biological activity towards parasites without strongly complexing with the anthelmintic, thereby maintaining good bioavailability or even enhancing it.

The next step could be the controlled addition of a limited number of variables, to stepwise approach the in vivo conditions possessing a great number of uncontrollable variables. This could be achieved by in vitro nematode trials with an emphasis on the use of pure and well-characterized model compounds, or by examining how the nature of direct interactions studied in this work changes with the introduction of different targets of tannins, such as macromolecules normally present at gut conditions, i.e., dietary proteins or polysaccharides. The plausible cooperative effects of tannins (and other natural compounds) should also be investigated in a separate study, as these effects most likely will take place when using tannin-rich forage or plant extracts. The in vitro trials with different helminth species could also include proteomics comparisons to gain a deeper understanding of how tannins affect the pharmacological effects of the introduced anthelmintic. Furthermore, these in vivo and in vitro approaches could also benefit from studies made in silico, for example involving molecular modelling and computational interaction studies.

To conclude, there is an urgent need to find novel helminth control strategies utilizing both medical and non-medical approaches and plant tannins could be viable candidates as more sustainable natural anthelmintics, while also inducing other beneficial effects. This work aimed to deepen our understanding of the molecular-level interactions between plant tannins and commercial anthelmintics as a step towards routine and deterministic inclusion of tannins in animal feeds. In this context, carefully selected tannins could enhance the effectiveness of administered anthelmintics, particularly in cases where resistance is emerging, but the anthelmintic still retains some efficacy. This is especially relevant in situations where no alternative anthelmintics are available, as seen with horses in Finland and sheep globally. The ultimate goal is that the results of this research can be utilized in future in vivo studies in implementing the principle of three Rs: replacement, reduction, and refinement.

Acknowledgements

This PhD work was conducted in the Natural Chemistry Research Group (NCRG) at the Department of Chemistry, University of Turku, during 2021–2025. The work was founded by the Finnish Research Council (LipidET, 310549), the University of Turku graduate school: Doctoral Programme in Exact Sciences (EXACTUS, previously PCS), NCRG, University of Turku Joint Research Grant Fund, the Finnish Concordia Fund, the Department of Chemistry, Orion Research Foundation, TOP Foundation, and the Foundation of Finnish Chemistry Congress. Thank you for making this research possible.

First, I want to thank Professor Francisco A. Macías and Research Professor Antti Oksanen for reviewing this work as pre-publication examiners – thank you for your encouraging and valuable comments. They truly did act as a further validation of this work in a time of need. I also wish to thank Research Director Carine Le Bourvellec for agreeing to act as my opponent for the doctoral dissertation.

Thank you, Professor Juha-Pekka Salminen, for introducing me to the wonderful world of plant chemistry and chemical analytics, starting all the way from the LY-kurssi. I sincerely appreciate the many opportunities you have provided, as they have had a paramount effect on how I view the world of analytical chemistry and what kind of chemist I have grown to be.

I am especially grateful to my supervisor, Docent Maarit Karonen, for your unwavering support throughout this journey. Your guidance and warmth over the years have impacted me immensely and the lessons I have had the privilege to learn from you, especially related to work-life balance, I will carry on into the future. Your enthusiastic, warm, and joyful presence is something that every workplace should have more of. Thank you for making such a positive impact on the lives of so many chemistry students, whether by supporting them through difficult times or simply spreading the joy of chemistry and analytics.

I also want to express my gratitude to my other supervisors, Docent Petri Tähtinen and Dr. Marica Engström. Petri, your deep knowledge and insight into the fundamentals of chemistry have been valuable through these years and I am grateful to have learnt from you. Thank you for all the help and guidance with NMR. Marica, thank you for acting as my supervisor for all these years, from the beginning of my

masters' work in 2018 all the way to the end of this PhD. You have (hopefully!) witnessed my growth as both a chemist and a person. Your teachings have acted as a foundation on how to conduct research and these are the building blocks this very work stands on. Thank you for all these years, for the humor you have spread and for all the support you have provided. Thank you for encouraging me to pursue this doctoral journey and I am truly glad you have been part of it.

I would like to thank Kari Loikas, Mauri Nauma, and Kirsi Laaksonen for their invaluable technical support during this work. The people at the Department of Chemistry are truly lucky to have you. Special thanks to Mauri for your help with the problems with the ITC syringe, without your help the data gathering for Articles I and II would have been terribly more expensive and delayed quite a bit.

My academic journey, from bachelor's to master's to PhD, has been filled with laughter and amazing coffee room discussions all thanks to the amazing current and former doctoral researchers in our research group. Thank you Dr. Jorma Kim, Dr. Milla Leppä, Dr. Marianna Manninen, Dr. Iqbal Bin Imran, Dr. Valtteri Virtanen, Dr. Juuso Laitila, Dr. Suvi Vanhakylä, Jussi Suvanto, Niko Luntamo, Ilari Kuukkanen, Ville Fock, and Bella Möller for sharing these moments with me. Anne Koivuniemi, thank you for joining me at Biocity to figure out the wonders of ITC – your presence was much needed at that time and during those weeks I got to know you much better than I had during my times as a summer or part-time employee. The days spent at Biocity also opened a door to another lifelong friendship; thank you Liisa Pösö for making those days so much less boring and lonely and for sharing the ups and downs of being a dog owner.

During these years I have also gotten invaluable peer support from my fellow doctoral student Anniina Jokela. Your company, and especially our weekly swims, have brough much needed balance especially during the final year of this PhD journey. Thank you for patiently listening to my rambling during those low moments.

I am grateful for all the friends made during my time at the university – thanks to you, I truly felt a sense of belonging when I first started my chemistry studies. Even though many of you have taken paths outside of chemistry, our friendships have still followed through. Thank you especially OBM: Laura, Emilia, Janita, Jenni, Ira, Krista, Antti, and Suvi-Anna for all the shared memories, past and future.

Äiti ja Iskä, I am deeply grateful for your unwavering support. You have always had more faith in me than I have had in myself, and it really has been a source of strength to know that I could rely on you whenever I truly needed help. I have never had to think twice about reaching out, whether in difficult moments or times of discouragement, because you have always been there, ready to listen, to guide, or simply to be present.

Lastly, I want to thank my partner Tuomas Räty for walking beside me through every high and low of this PhD journey. These years have not been the easiest, but we have pushed them through. It has been an absolute joy to have a fellow chemist to share this journey with, as you have listened to my frustrations, discussed the beautiful world of chemistry with me, and helped with the practicalities of NMR. Also, thank you for always reminding me that life is not only defined by the length of a checked to-do list, but also by knowing when to pause and enjoy the moments of peace and quiet. Thank you for being someone I can always count on.

August 2025, Turku

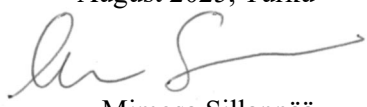

Mimosa Sillanpää

List of References

(1) Mueller-Harvey, I. Unravelling the Conundrum of Tannins in Animal Nutrition and Health. *J. Sci. Food Agric.* **2006**, *86* (13), 2010–2037. https://doi.org/10.1002/jsfa.2577.

(2) Min, B. R.; Hart, S. P.; Miller, D.; Tomita, G. M.; Loetz, E.; Sahlu, T. The Effect of Grazing Forage Containing Condensed Tannins on Gastro-Intestinal Parasite Infection and Milk Composition in Angora Does. *Vet. Parasitol.* **2005**, *130* (1–2), 105–113. https://doi.org/10.1016/J.VETPAR.2005.03.011.

(3) Waghorn, G. C.; McNabb, W. C. Consequences of Plant Phenolic Compounds for Productivity and Health of Ruminants. *Proc. Nutr. Soc.* **2003**, *62* (2), 383–392. https://doi.org/10.1079/pns2003245.

(4) Hatano, T.; Kusuda, M.; Inada, K.; Ogawa, T. O.; Shiota, S.; Tsuchiya, T.; Yoshida, T. Effects of Tannins and Related Polyphenols on Methicillin-Resistant *Staphylococcus Aureus*. In *Phytochemistry*; Pergamon, 2005; Vol. 66, pp 2047–2055. https://doi.org/10.1016/j.phytochem.2005.01.013.

(5) Jakobek, L. Interactions of Polyphenols with Carbohydrates, Lipids and Proteins. *Food Chem.* **2015**, *175*, 556–567. https://doi.org/10.1016/J.FOODCHEM.2014.12.013.

(6) Baert, N.; Pellikaan, W. F.; Karonen, M.; Salminen, J.-P. A Study of the Structure-Activity Relationship of Oligomeric Ellagitannins on Ruminal Fermentation in Vitro. *J. Dairy Sci.* **2016**, *99* (10), 8041–8052. https://doi.org/10.3168/JDS.2016-11069.

(7) Hagerman, A. E. Fifty Years of Polyphenol-Protein Complexes. In *Recent Advances in Polyphenol Research, Volume 3*; Wiley-Blackwell, 2012; Vol. 3, pp 71–97. https://doi.org/10.1002/9781118299753.ch3.

(8) Gontijo, D. C.; Gontijo, P. C.; Brandão, G. C.; Diaz, M. A. N.; de Oliveira, A. B.; Fietto, L. G.; Leite, J. P. V. Antioxidant Study Indicative of Antibacterial and Antimutagenic Activities of an Ellagitannin-Rich Aqueous Extract from the Leaves of *Miconia Latecrenata*. *J. Ethnopharmacol.* **2019**, *236*, 114–123. https://doi.org/10.1016/J.JEP.2019.03.007.

(9) Moilanen, J.; Salminen, J. P. Ecologically Neglected Tannins and Their Biologically Relevant Activity: Chemical Structures of Plant Ellagitannins Reveal Their in Vitro Oxidative Activity at High PH. *Chemoecology* **2008**, *18* (2), 73–83. https://doi.org/10.1007/s00049-007-0395-7.

(10) Barbehenn, R. V.; Jones, C. P.; Hagerman, A. E.; Karonen, M.; Salminen, J. P. Ellagitannins Have Greater Oxidative Activities than Condensed Tannins and Galloyl Glucoses at High PH: Potential Impact on Caterpillars. *J. Chem. Ecol.* **2006**, *32* (10), 2253–2267. https://doi.org/10.1007/s10886-006-9143-7.

(11) Virtanen, V.; Räikkönen, S.; Puljula, E.; Karonen, M. Ellagitannin–Lipid Interaction by HR-MAS NMR Spectroscopy. *Molecules* **2021**, *26* (2), 373. https://doi.org/10.3390/molecules26020373.

(12) Karonen, M. Insights into Polyphenol–Lipid Interactions: Chemical Methods, Molecular Aspects and Their Effects on Membrane Structures. *Plants* **2022**, *11* (14), 1809. https://doi.org/10.3390/plants11141809.

(13) Le Bourvellec, C.; Renard, C. M. G. C. Interactions between Polyphenols and Macromolecules: Quantification Methods and Mechanisms. *Crit. Rev. Food Sci. Nutr.* **2012**, *52* (3), 213–248. https://doi.org/10.1080/10408398.2010.499808.

(14) Renard, C. M. G. C.; Baron, A.; Guyot, S.; Drilleau, J. F. Interactions between Apple Cell Walls and Native Apple Polyphenols: Quantification and Some Consequences. *Int. J. Biol. Macromol.* **2001**, *29* (2), 115–125. https://doi.org/10.1016/S0141-8130(01)00155-6.

(15) Puljula, E.; Walton, G.; Woodward, M. J.; Karonen, M. Antimicrobial Activities of Ellagitannins against *Clostridiales Perfringens*, *Escherichia Coli*, *Lactobacillus Plantarum* and *Staphylococcus Aureus*. *Molecules* **2020**, *25* (16), 3714. https://doi.org/10.3390/molecules25163714.

(16) Scalbert, A. *Antimicrobial Properties of Tannins*; Pergamon, 1991; Vol. 30, pp 3875–3883. https://doi.org/10.1016/0031-9422(91)83426-L.

(17) Brunet, S.; Hoste, H. Monomers of Condensed Tannins Affect the Larval Exsheathment of Parasitic Nematodes of Ruminants. *J. Agric. Food Chem.* **2006**, *54* (20), 7481–7487.

(18) Engström, M. T.; Karonen, M.; Ahern, J. R.; Baert, N.; Payré, B.; Hoste, H.; Salminen, J.-P. Chemical Structures of Plant Hydrolyzable Tannins Reveal Their in Vitro Activity against Egg Hatching and Motility of *Haemonchus Contortus* Nematodes. *J. Agric. Food Chem.* **2016**, *64* (4), 840–851. https://doi.org/10.1021/acs.jafc.5b05691.

(19) Molan, A. L.; Hoskin, S. O.; Barry, T. N.; McNabb, W. C. Effect of Condensed Tannins Extracted from Four Forages on the Viability of the Larvae of Deer Lungworms and Gastrointestinal Nematodes. *Vet. Rec.* **2000**, *147* (2), 44–48. https://doi.org/10.1136/VR.147.2.44.

(20) Karonen, M.; Ahern, J. R.; Legroux, L.; Suvanto, J.; Engström, M. T.; Sinkkonen, J.; Salminen, J. P.; Hoste, H. Ellagitannins Inhibit the Exsheathment of *Haemonchus Contortus* and *Trichostrongylus Colubriformis* Larvae: The Efficiency Increases Together with the Molecular Size. *J. Agric. Food Chem.* **2020**, *68* (14), 4176–4186. https://doi.org/10.1021/acs.jafc.9b06774.

(21) Okuda, T.; Yoshida, T.; Hatano, T. Classification of Oligomeric Hydrolysable Tannins and Specificity of Their Occurrence in Plants. *Phytochemistry* **1993**, *32* (3), 507–521. https://doi.org/10.1016/S0031-9422(00)95129-X.

(22) Esatbeyoglu, T.; Winterhalter, P. Preparation of Dimeric Procyanidins B1, B2, B5, and B7 from a Polymeric Procyanidin Fraction of Black Chokeberry (*Aronia Melanocarpa*). *J. Agric. Food Chem.* **2010**, *58* (8), 5147–5153. https://doi.org/10.1021/jf904354n.

(23) Esatbeyoglu, T.; Wray, V.; Winterhalter, P. Isolation of Dimeric, Trimeric, Tetrameric and Pentameric Procyanidins from Unroasted Cocoa Beans (*Theobroma Cacao* L.) Using Countercurrent Chromatography. *Food Chem.* **2015**, *179*, 278–289. https://doi.org/10.1016/J.FOODCHEM.2015.01.130.

(24) Ito, C.; Oki, T.; Yoshida, T.; Nanba, F.; Yamada, K.; Toda, T. Characterisation of Proanthocyanidins from Black Soybeans: Isolation and Characterisation of Proanthocyanidin Oligomers from Black Soybean Seed Coats. *Food Chem.* **2013**, *141* (3), 2507–2512. https://doi.org/10.1016/J.FOODCHEM.2013.05.039.

(25) Köhler, N.; Wray, V.; Winterhalter, P. Preparative Isolation of Procyanidins from Grape Seed Extracts by High-Speed Counter-Current Chromatography. *J. Chromatogr. A* **2008**, *1177* (1), 114–125. https://doi.org/10.1016/j.chroma.2007.11.028.

(26) Leppä, M. M.; Karonen, M.; Tähtinen, P.; Engström, M. T.; Salminen, J.-P. Isolation of Chemically Well-Defined Semipreparative Liquid Chromatography Fractions from Complex Mixtures of Proanthocyanidin Oligomers and Polymers. *J. Chromatogr. A* **2018**, *1576*, 67–79. https://doi.org/10.1016/j.chroma.2018.09.034.

(27) Liimatainen, J.; Karonen, M.; Sinkkonen, J. Procyanidin Xylosides from the Bark of Betula Pendula. *Phytochemistry* **2012**, *76*, 178–183. https://doi.org/10.1016/j.phytochem.2012.01.008.

(28) Kaplan, R. M. Drug Resistance in Nematodes of Veterinary Importance: A Status Report. *Trends Parasitol.* **2004**, *20* (10), 477–481. https://doi.org/10.1016/j.pt.2004.08.001.

(29) Kaplan, R. M.; Vidyashankar, A. N. An Inconvenient Truth: Global Worming and Anthelmintic Resistance. *Vet. Parasitol.* **2012**, *186* (1–2), 70–78. https://doi.org/10.1016/J.VETPAR.2011.11.048.

(30) Rose, H.; Rinaldi, L.; Bosco, A.; Mavrot, F.; De Waal, T.; Skuce, P.; Charlier, J.; Torgerson, P. R.; Hertzberg, H.; Hendrickx, G.; Vercruysse, J.; Morgan, E. R. Widespread Anthelmintic Resistance in European Farmed Ruminants: A Systematic Review. *Vet. Rec.* **2015**, *176* (21), 546. https://doi.org/10.1136/VR.102982/-/DC1.

(31) Rose Vineer, H.; Morgan, E. R.; Hertzberg, H.; Bartley, D. J.; Bosco, A.; Charlier, J.; Chartier, C.; Claerebout, E.; De Waal, T.; Hendrickx, G.; Hinney, B.; Höglund, J.; Jez Ek, J. I.; Kašný, M.; Keane, O. M.; Martínez-Valladares, M.; Mateus, T. L.; McIntyre, J.; Mickiewicz, M.; Munoz, A. M.; Phythian, C. J.; Ploeger, H. W.; Rataj, A. V.; Skuce, P. J.; Simin, S.; Sotiraki, S.; Spinu, M.; Stuen, S.; Thamsborg, S. M.; Vadlejch, J.; Varady, M.; Von Samson-Himmelstjerna, G.; Rinaldi, L. Increasing Importance of Anthelmintic Resistance in European Livestock: Creation and Meta-Analysis of an Open Database. *Parasite* **2020**, *27*. https://doi.org/10.1051/PARASITE/2020062.

(32) Ahuir-Baraja, A. E.; Cibot, F.; Llobat, L.; Garijo, M. M. Anthelmintic Resistance: Is a Solution Possible? *Exp. Parasitol.* **2021**, *230*, 108169. https://doi.org/10.1016/J.EXPPARA.2021.108169.

(33) Kaplan, R. M. Biology, Epidemiology, Diagnosis, and Management of Anthelmintic Resistance in Gastrointestinal Nematodes of Livestock. *Vet. Clin. North Am. Food Anim. Pract.* **2020**, *36* (1), 17–30. https://doi.org/10.1016/J.CVFA.2019.12.001.

(34) Burke, J. M.; Miller, J. E.; Terrill, T. H. Impact of Rotational Grazing on Management of Gastrointestinal Nematodes in Weaned Lambs. *Vet. Parasitol.* **2009**, *163* (1–2), 67–72. https://doi.org/10.1016/J.VETPAR.2009.03.054.

(35) Shalaby, H. A. Anthelmintics Resistance; How to Overcome It? *Iran. J. Parasitol.* **2013**, *8* (1), 18.

(36) Hoste, H.; Martinez-Ortiz-De-Montellano, C.; Manolaraki, F.; Brunet, S.; Ojeda-Robertos, N.; Fourquaux, I.; Torres-Acosta, J. F. J.; Sandoval-Castro, C. A. Direct and Indirect Effects of Bioactive Tannin-Rich Tropical and Temperate Legumes against Nematode Infections. *Vet. Parasitol.* **2012**, *186* (1–2), 18–27. https://doi.org/10.1016/j.vetpar.2011.11.042.

(37) Waghorn, G. C.; Ulyatt, M. J.; John, A.; Fisher, M. T. The Effect of Condensed Tannins on the Site of Digestion of Amino Acids and Other Nutrients in Sheep Fed on *Lotus Corniculatus* L. *Br. J. Nutr.* **1987**, *57* (1), 115–126. https://doi.org/10.1079/bjn19870015.

(38) Mueller-Harvey, I.; Bee, G.; Dohme-Meier, F.; Hoste, H.; Karonen, M.; Kölliker, R.; Lüscher, A.; Niderkorn, V.; Pellikaan, W. F.; Salminen, J. P.; Skøt, L.; Smith, L. M. J.; Thamsborg, S. M.; Totterdell, P.; Wilkinson, I.; Williams, A. R.; Azuhnwi, B. N.; Baert, N.; Brinkhaus, A. G.; Copani, G.; Desrues, O.; Drake, C.; Engström, M.; Fryganas, C.; Girard, M.; Huyen, N. T.; Kempf, K.; Malisch, C.; Mora-Ortiz, M.; Quijada, J.; Ramsay, A.; Ropiak, H. M.; Waghorn, G. C. Benefits of Condensed Tannins in Forage Legumes Fed to Ruminants: Importance of Structure, Concentration, and Diet Composition. *Crop Sci.* **2019**, *59* (3), 861–885. https://doi.org/10.2135/cropsci2017.06.0369.

(39) Min, B. R.; McNabb, W. C.; Barry, T. N.; Peters, J. S. Solubilization and Degradation of Ribulose-1,5-Bisphosphate Carboxylase/Oxygenase (EC 4.1.1.39; Rubisco) Protein from White Clover (*Trifolium Repens*) and *Lotus Corniculatus* by Rumen Microorganisms and the Effect of Condensed Tannins on These. *J. Agric. Sci.* **2000**, *134* (3), 305–317. https://doi.org/10.1017/S0021859699007698.

(40) Aerts, R. J.; Barry, T. N.; McNabb, W. C. Polyphenols and Agriculture: Beneficial Effects of Proanthocyanidins in Forages. *Agric. Ecosyst. Environ.* **1999**, *75* (1–2), 1–12. https://doi.org/10.1016/S0167-8809(99)00062-6.

(41) Jones, W. T.; Mangan, J. L. Complexes of the Condensed Tannins of Sainfoin (Onobrychis Viciifolia Scop.) with Fraction 1 Leaf Protein and with Submaxillary Mucoprotein, and Their

Reversal by Polyethylene Glycol and PH. *J. Sci. Food Agric.* **1977**, *28* (2), 126–136. https://doi.org/10.1002/JSFA.2740280204.

(42) Patra, A. K.; Saxena, J. Exploitation of Dietary Tannins to Improve Rumen Metabolism and Ruminant Nutrition. *J. Sci. Food Agric.* **2011**, *91* (1), 24–37. https://doi.org/10.1002/JSFA.4152.

(43) Quijada, J.; Drake, C.; Gaudin, E.; El-Korso, R.; Hoste, H.; Mueller-Harvey, I. Condensed Tannin Changes along the Digestive Tract in Lambs Fed with Sainfoin Pellets or Hazelnut Skins. *J. Agric. Food Chem.* **2018**, *66* (9), 2136–2142. https://doi.org/10.1021/acs.jafc.7b05538.

(44) Girard, M.; Lehtimäki, A.; Bee, G.; Dohme-Meier, F.; Karonen, M.; Salminen, J.-P. Changes in Feed Proanthocyanidin Profiles during Silage Production and Digestion by Lamb. *Molecules* **2020**, *25* (24), 5887. https://doi.org/10.3390/molecules25245887.

(45) Desrues, O.; Mueller-Harvey, I.; Pellikaan, W. F.; Enemark, H. L.; Thamsborg, S. M. Condensed Tannins in the Gastrointestinal Tract of Cattle after Sainfoin (*Onobrychis Viciifolia*) Intake and Their Possible Relationship with Anthelmintic Effects. *J. Agric. Food Chem.* **2017**, *65* (7), 1420–1427. https://doi.org/10.1021/acs.jafc.6b05830.

(46) Kilmister, R. L.; Faulkner, P.; Downey, M. O.; Darby, S. J.; Falconer, R. J. The Complexity of Condensed Tannin Binding to Bovine Serum Albumin - An Isothermal Titration Calorimetry Study. *Food Chem.* **2016**, *190*, 173–178. https://doi.org/10.1016/j.foodchem.2015.04.144.

(47) Baxter, N. J.; Lilley, T. H.; Haslam, E.; Williamson, M. P. Multiple Interactions between Polyphenols and a Salivary Proline-Rich Protein Repeat Result in Complexation and Precipitation. *Biochemistry* **1997**, *36* (18), 5566–5577. https://doi.org/10.1021/bi9700328.

(48) Harbertson, J. F.; Kilmister, R. L.; Kelm, M. A.; Downey, M. O. Impact of Condensed Tannin Size as Individual and Mixed Polymers on Bovine Serum Albumin Precipitation. *Food Chem.* **2014**, *160*, 16–21. https://doi.org/10.1016/j.foodchem.2014.03.026.

(49) Soares, S.; García-Estévez, I.; Ferrer-Galego, R.; Brás, N. F.; Brandão, E.; Silva, M.; Teixeira, N.; Fonseca, F.; Sousa, S. F.; Ferreira-da-Silva, F.; Mateus, N.; de Freitas, V. Study of Human Salivary Proline-Rich Proteins Interaction with Food Tannins. *Food Chem.* **2018**, *243*, 175–185. https://doi.org/10.1016/j.foodchem.2017.09.063.

(50) De Freitas, V.; Mateus, N. Structural Features of Procyanidin Interactions with Salivary Proteins. *J. Agric. Food Chem.* **2001**, *49* (2), 940–945. https://doi.org/10.1021/jf000981z.

(51) Leppä, M. M.; Laitila, J. E.; Salminen, J.-P. Distribution of Protein Precipitation Capacity within Variable Proanthocyanidin Fingerprints. *Molecules* **2020**, *25* (21), 5002. https://doi.org/10.3390/molecules25215002.

(52) Zeller, W. E.; Reinhardt, L. A.; Robe, J. T.; Sullivan, M. L.; Panke-Buisse, K. Comparison of Protein Precipitation Ability of Structurally Diverse Procyanidin-Rich Condensed Tannins in Two Buffer Systems. *J. Agric. Food Chem.* **2020**, *68* (7), 2016–2023. https://doi.org/10.1021/ACS.JAFC.9B06173.

(53) Kimura, H.; Ogawa, S.; Akihiro, T.; Yokota, K. Structural Analysis of A-Type or B-Type Highly Polymeric Proanthocyanidins by Thiolytic Degradation and the Implication in Their Inhibitory Effects on Pancreatic Lipase. *J. Chromatogr. A* **2011**, *1218* (42), 7704–7712. https://doi.org/10.1016/J.CHROMA.2011.07.024.

(54) Zhu, W.; Xiong, L.; Peng, J.; Deng, X.; Gao, J.; Li, C. M. Molecular Insight into Affinities of Gallated and Nongallated Proanthocyanidins Dimers to Lipid Bilayers. *Sci. Rep.* **2016**, *6* (1), 1–13. https://doi.org/10.1038/srep37680.

(55) Zhu, W.; Wang, R. F.; Khalifa, I.; Li, C. M. Understanding toward the Biophysical Interaction of Polymeric Proanthocyanidins (Persimmon Condensed Tannins) with Biomembranes: Relevance for Biological Effects. *J. Agric. Food Chem.* **2019**, *67* (40), 11044–11052. https://doi.org/10.1021/acs.jafc.9b04508.

(56) Zhu, W.; Zou, B.; Nie, R.; Zhang, Y.; Li, C. M. A-Type ECG and EGCG Dimers Disturb the Structure of 3T3-L1 Cell Membrane and Strongly Inhibit Its Differentiation by Targeting Peroxisome Proliferator-Activated Receptor γ with MiR-27 Involved Mechanism. *J. Nutr. Biochem.* **2015**, *26* (11), 1124–1135. https://doi.org/10.1016/j.jnutbio.2015.05.006.

(57) Verstraeten, S. V.; Keen, C. L.; Schmitz, H. H.; Fraga, C. G.; Oteiza, P. I. Flavan-3-Ols and Procyanidins Protect Liposomes against Lipid Oxidation and Disruption of the Bilayer Structure. *Free Radic. Biol. Med.* **2003**, *34* (1), 84–92. https://doi.org/10.1016/S0891-5849(02)01185-1.

(58) Desrues, O.; Fryganas, C.; Ropiak, H. M.; Mueller-Harvey, I.; Enemark, H. L.; Thamsborg, S. M. Impact of Chemical Structure of Flavanol Monomers and Condensed Tannins on in Vitro Anthelmintic Activity against Bovine Nematodes. *Parasitology* **2016**, *143* (4), 444–454. https://doi.org/10.1017/S0031182015001912.

(59) Quijada, J.; Fryganas, C.; Ropiak, H. M.; Ramsay, A.; Mueller-Harvey, I.; Hoste, H. Anthelmintic Activities against *Haemonchus Contortus* or *Trichostrongylus Colubriformis* from Small Ruminants Are Influenced by Structural Features of Condensed Tannins. *J. Agric. Food Chem.* **2015**, *63* (28), 6346–6354. https://doi.org/10.1021/ACS.JAFC.5B00831.

(60) Ramsay, A.; Williams, A. R.; Thamsborg, S. M.; Mueller-Harvey, I. Galloylated Proanthocyanidins from Shea (*Vitellaria Paradoxa*) Meal Have Potent Anthelmintic Activity against *Ascaris Suum*. *Phytochemistry* **2016**, *122*, 146–153. https://doi.org/10.1016/j.phytochem.2015.12.005.

(61) Karonen, M.; Oraviita, M.; Mueller-Harvey, I.; Salminen, J.-P.; Green, R. J. Binding of an Oligomeric Ellagitannin Series to Bovine Serum Albumin (BSA): Analysis by Isothermal Titration Calorimetry (ITC). *J. Agric. Food Chem* **2015**, *63*, 9. https://doi.org/10.1021/acs.jafc.5b04843.

(62) Karonen, M.; Oraviita, M.; Mueller-Harvey, I.; Salminen, J.-P.; Green, R. J. Ellagitannins with Glucopyranose Cores Have Higher Affinities to Proteins than Acyclic Ellagitannins by Isothermal Titration Calorimetry. *J. Agric. Food Chem.* **2019**, *67* (46), 12730–12740. https://doi.org/10.1021/acs.jafc.9b04353.

(63) Deaville, E. R.; Green, R. J.; Mueller-Harvey, I.; Willoughby, I.; Frazier, R. A. Hydrolyzable Tannin Structures Influence Relative Globular and Random Coil Protein Binding Strengths. *J. Agric. Food Chem.* **2007**, *55* (11), 4554–4561. https://doi.org/10.1021/jf063770o.

(64) Dobreva, M. A.; Green, R. J.; Mueller-Harvey, I.; Salminen, J.-P.; Howlin, B. J.; Frazier, R. A. Size and Molecular Flexibility Affect the Binding of Ellagitannins to Bovine Serum Albumin. *J. Agric. Food Chem.* **2014**, *62* (37), 9186–9194. https://doi.org/10.1021/jf502174r.

(65) Virtanen, V.; Green, R. J.; Karonen, M. Interactions between Hydrolysable Tannins and Lipid Vesicles from *Escherichia Coli* with Isothermal Titration Calorimetry. *Molecules* **2022**, *27* (10), 3204. https://doi.org/10.3390/MOLECULES27103204.

(66) Zajac, A. M. Gastrointestinal Nematodes of Small Ruminants: Life Cycle, Anthelmintics, and Diagnosis. *Vet. Clin. North Am. - Food Anim. Pract.* **2006**, *22* (3), 529–541. https://doi.org/10.1016/j.cvfa.2006.07.006.

(67) Williams, A. R.; Ropiak, H. M.; Fryganas, C.; Desrues, O.; Mueller-Harvey, I.; Thamsborg, S. M. Assessment of the Anthelmintic Activity of Medicinal Plant Extracts and Purified Condensed Tannins against Free-Living and Parasitic Stages of *Oesophagostomum Dentatum*. *Parasit. Vectors* **2014**, *7* (1). https://doi.org/10.1186/S13071-014-0518-2.

(68) Hoste, H.; Jackson, F.; Athanasiadou, S.; Thamsborg, S. M.; Hoskin, S. O. The Effects of Tannin-Rich Plants on Parasitic Nematodes in Ruminants. *Trends Parasitol.* **2006**, *22* (6), 253–261. https://doi.org/10.1016/j.pt.2006.04.004.

(69) Martínez-Ortíz-de-Montellano, C.; Arroyo-López, C.; Fourquaux, I.; Torres-Acosta, J. F. J.; Sandoval-Castro, C. A.; Hoste, H. Scanning Electron Microscopy of *Haemonchus Contortus* Exposed to Tannin-Rich Plants under *in Vivo* and *in Vitro* Conditions. *Exp. Parasitol.* **2013**, *133* (3), 281–286. https://doi.org/10.1016/j.exppara.2012.11.024.

(70) Desrues, O.; Peña-Espinoza, M.; Hansen, T. V. A.; Enemark, H. L.; Thamsborg, S. M. Anti-Parasitic Activity of Pelleted Sainfoin (*Onobrychis Viciifolia*) against *Ostertagia Ostertagi* and *Cooperia Oncophora* in Calves. *Parasites and Vectors* **2016**, *9* (1), 1–10. https://doi.org/10.1186/s13071-016-1617-z.

(71) Terrill, T. H.; Dykes, G. S.; Shaik, S. A.; Miller, J. E.; Kouakou, B.; Kannan, G.; Burke, J. M.; Mosjidis, J. A. Efficacy of Sericea Lespedeza Hay as a Natural Dewormer in Goats: Dose Titration Study. *Vet. Parasitol.* **2009**, *163* (1–2), 52–56. https://doi.org/10.1016/J.VETPAR.2009.04.022.

(72) Shaik, S. A.; Terrill, T. H.; Miller, J. E.; Kouakou, B.; Kannan, G.; Kaplan, R. M.; Burke, J. M.; Mosjidis, J. A. Sericea Lespedeza Hay as a Natural Deworming Agent against Gastrointestinal Nematode Infection in Goats. *Vet. Parasitol.* **2006**, *139* (1–3), 150–157. https://doi.org/10.1016/j.vetpar.2006.02.020.

(73) Heckendorn, F.; Häring, D. A.; Maurer, V.; Senn, M.; Hertzberg, H. Individual Administration of Three Tanniferous Forage Plants to Lambs Artificially Infected with *Haemonchus Contortus* and *Cooperia Curticei*. *Vet. Parasitol.* **2007**, *146* (1–2), 123–134. https://doi.org/10.1016/j.vetpar.2007.01.009.

(74) Heckendorn, F.; Häring, D. A.; Maurer, V.; Zinsstag, J.; Langhans, W.; Hertzberg, H. Effect of Sainfoin (*Onobrychis Viciifolia*) Silage and Hay on Established Populations of *Haemonchus Contortus* and *Cooperia Curticei* in Lambs. *Vet. Parasitol.* **2006**, *142* (3–4), 293–300. https://doi.org/10.1016/J.VETPAR.2006.07.014.

(75) Waghorn, G. C.; Waghorn, T. S. Growth and Gastrointestinal Nematode Parasitism in Lambs Grazing Either Lucerne (*Medicago Sativa*) or Sulla (*Hedysarum Coronarium*) Which Contains Condensed Tannins. *J. Agric. Sci.* **1995**, *125* (2), 281–289. https://doi.org/10.1017/S0021859600084422.

(76) Niezen, J. H.; Waghorn, G. C.; Charleston, W. A. G. Establishment and Fecundity of *Ostertagia Circumcincta* and *Trichostrongylus Colubriformis* in Lambs Fed Lotus (*Lotus Pedunculatus*) or Perennial Ryegrass (*Lolium Perenne*). *Vet. Parasitol.* **1998**, *78* (1), 13–21. https://doi.org/10.1016/S0304-4017(98)00121-6.

(77) Paolini, V.; Frayssines, A.; De, F.; Farge, L. A.; Dorchies, P.; Hoste, H. Effects of Condensed Tannins on Established Populations and on Incoming Larvae of Trichostrongylus Colubriformis and Teladorsagia Circumcincta in Goats. *Vet. Res.* **2003**, *34*, 1–9. https://doi.org/10.1051/vetres:2003008.

(78) Brunet, S.; Montellano, C. M. O. de; Torres-Acosta, J. F. J.; Sandoval-Castro, C. A.; Aguilar-Caballero, A. J.; Capetillo-Leal, C.; Hoste, H. Effect of the Consumption of *Lysiloma Latisiliquum* on the Larval Establishment of Gastrointestinal Nematodes in Goats. *Vet. Parasitol.* **2008**, *157* (1–2), 81–88. https://doi.org/10.1016/j.vetpar.2008.07.013.

(79) Brunet, S.; Aufrere, J.; El Babili, F.; Fouraste, I.; Hoste, H. The Kinetics of Exsheathment of Infective Nematode Larvae Is Disturbed in the Presence of a Tannin-Rich Plant Extract (Sainfoin) Both in Vitro and in Vivo. *Parasitology* **2007**, *134* (9), 1253–1262. https://doi.org/10.1017/S0031182007002533.

(80) Athanasiadou, S.; Kyriazakis, I.; Jackson, F.; Coop, R. L. Direct Anthelmintic Effects of Condensed Tannins towards Different Gastrointestinal Nematodes of Sheep: In Vitro and in Vivo Studies. *Vet. Parasitol.* **2001**, *99* (3), 205–219. https://doi.org/10.1016/S0304-4017(01)00467-8.

(81) Azuhnwi, B. N.; Hertzberg, H.; Arrigo, Y.; Gutzwiller, A.; Hess, H. D.; Mueller-Harvey, I.; Torgerson, P. R.; Kreuzer, M.; Dohme-Meier, F. Investigation of Sainfoin (*Onobrychis Viciifolia*) Cultivar Differences on Nitrogen Balance and Fecal Egg Count in Artificially Infected Lambs. *J. Anim. Sci.* **2013**, *91* (5), 2343–2354. https://doi.org/10.2527/JAS.2012-5351.

(82) Komáromyová, M.; Petrič, D.; Kucková, K.; Batt'ányi, D.; Babják, M.; Dolinská, M. U.; Königová, A.; Barčák, D.; Dvorožňáková, E.; Čobanová, K.; Váradyová, Z.; Várady, M. Impact of Sainfoin (*Onobrychis Viciifolia*) Pellets on Parasitological Status, Antibody Responses, and Antioxidant Parameters in Lambs Infected with *Haemonchus Contortus*. *Pathogens* **2022**, *11* (3), 301. https://doi.org/10.3390/pathogens11030301.

(83) Katiki, L. M.; Gomes, A. C. P.; Barbieri, A. M. E.; Pacheco, P. A.; Rodrigues, L.; Veríssimo, C. J.; Gutmanis, G.; Piza, A. M.; Louvandini, H.; Ferreira, J. F. S. *Terminalia Catappa*: Chemical

Composition, *in Vitro* and *in Vivo* Effects on *Haemonchus Contortus*. *Vet. Parasitol.* **2017**, *246*, 118–123. https://doi.org/10.1016/j.vetpar.2017.09.006.

(84) Lanusse, C.; Canton, C.; Virkel, G.; Alvarez, L.; Costa-Junior, L.; Lifschitz, A. Strategies to Optimize the Efficacy of Anthelmintic Drugs in Ruminants. *Trends Parasitol.* **2018**, *34* (8), 664–682. https://doi.org/10.1016/j.pt.2018.05.005.

(85) Silva, C. R.; Lifschitz, A. L.; Macedo, S. R. D.; Campos, N. R. C. L.; Viana-Filho, M.; Alcântara, A. C. S.; Araújo, J. G.; Alencar, L. M. R.; Costa-Junior, L. M. Combination of Synthetic Anthelmintics and Monoterpenes: Assessment of Efficacy, and Ultrastructural and Biophysical Properties of *Haemonchus Contortus* Using Atomic Force Microscopy. *Vet. Parasitol.* **2021**, *290*, 109345. https://doi.org/10.1016/J.VETPAR.2021.109345.

(86) Whitney, T. R.; Lupton, C. J.; Muir, J. P.; Adams, R. P.; Stewart, W. C. Effects of Using Ground Redberry Juniper and Dried Distillers Grains with Solubles in Lamb Feedlot Diets: Growth, Blood Serum, Fecal, and Wool Characteristics. *J. Anim. Sci.* **2014**, *92* (3), 1119–1132. https://doi.org/10.2527/JAS.2013-7007.

(87) Dupuy, J.; Larrieu, G.; Sutra, J. F.; Lespine, A.; Alvinerie, M. Enhancement of Moxidectin Bioavailability in Lamb by a Natural Flavonoid: Quercetin. *Vet. Parasitol.* **2003**, *112* (4), 337–347. https://doi.org/10.1016/S0304-4017(03)00008-6.

(88) Miró, M. V.; Luque, S.; Cardozo, P.; Lloberas, M.; Sousa, D. M.; Soares, A. M. S.; Costa-Junior, L. M.; Virkel, G. L.; Lifschitz, A. L. Plant-Derived Compounds as a Tool for the Control of Gastrointestinal Nematodes: Modulation of Abamectin Pharmacological Action by Carvone. *Front. Vet. Sci.* **2020**, *7*, 601750. https://doi.org/10.3389/fvets.2020.601750.

(89) Hansen, T. V. A.; Fryganas, C.; Acevedo, N.; Caraballo, L.; Thamsborg, S. M.; Mueller-Harvey, I.; Williams, A. R. Proanthocyanidins Inhibit *Ascaris Suum* Glutathione-S-Transferase Activity and Increase Susceptibility of Larvae to Levamisole in Vitro. *Parasitol. Int.* **2016**, *65* (4), 336–339. https://doi.org/10.1016/j.parint.2016.04.001.

(90) Armstrong, S. A.; Klein, D. R.; Whitney, T. R.; Scott, C. B.; Muir, J. P.; Lambert, B. D.; Craig, T. M. Effect of Using Redberry Juniper (*Juniperus Pinchotii*) to Reduce *Haemonchus Contortus* in Vitro Motility and Increase Ivermectin Efficacy. *Vet. Parasitol.* **2013**, *197* (1–2), 271–276. https://doi.org/10.1016/j.vetpar.2013.04.021.

(91) Miró, M. V.; e Silva, C. R.; Viviani, P.; Luque, S.; Lloberas, M.; Costa-Júnior, L. M.; Lanusse, C.; Virkel, G.; Lifschitz, A. Combination of Bioactive Phytochemicals and Synthetic Anthelmintics: *In Vivo* and *in Vitro* Assessment of the Albendazole-Thymol Association. *Vet. Parasitol.* **2020**, *281*, 109121. https://doi.org/10.1016/j.vetpar.2020.109121.

(92) Malsa, J.; Courtot, É.; Boisseau, M.; Dumont, B.; Gombault, P.; Kuzmina, T. A.; Basiaga, M.; Lluch, J.; Annonay, G.; Dhorne-Pollet, S.; Mach, N.; Sutra, J. F.; Wimel, L.; Dubois, C.; Guégnard, F.; Serreau, D.; Lespine, A.; Sallé, G.; Fleurance, G. Effect of Sainfoin (*Onobrychis Viciifolia*) on Cyathostomin Eggs Excretion, Larval Development, Larval Community Structure and Efficacy of Ivermectin Treatment in Horses. *Parasitology* **2022**, *149* (11), 1439. https://doi.org/10.1017/S0031182022000853.

(93) Gaudin, E.; Simon, M.; Quijada, J.; Schelcher, F.; Sutra, J. F.; Lespine, A.; Hoste, H. Efficacy of Sainfoin (*Onobrychis Viciifolia*) Pellets against Multi Resistant *Haemonchus Contortus* and Interaction with Oral Ivermectin: Implications for on-Farm Control. *Vet. Parasitol.* **2016**, *227*, 122–129. https://doi.org/10.1016/j.vetpar.2016.08.002.

(94) Whitney, T. R.; Wildeus, S.; Zajac, A. M. The Use of Redberry Juniper (*Juniperus Pinchotii*) to Reduce *Haemonchus Contortus* Fecal Egg Counts and Increase Ivermectin Efficacy. *Vet. Parasitol.* **2013**, *197* (1–2), 182–188. https://doi.org/10.1016/j.vetpar.2013.06.010.

(95) Villalaín, J. Epigallocatechin-3-Gallate Location and Interaction with Late Endosomal and Plasma Membrane Model Membranes by Molecular Dynamics. *J. Biomol. Struct. Dyn.* **2019**, *37* (12), 3122–3134. https://doi.org/10.1080/07391102.2018.1508372.

(96) Nakayama, T.; Hashimoto, T.; Kajiya, K.; Kumazawa, S. Affinity of Polyphenols for Lipid Bilayers. *BioFactors* **2000**, *13* (1–4), 147–151. https://doi.org/10.1002/biof.5520130124.

(97) Furlan, A. L.; Jobin, M. L.; Buchoux, S.; Grélard, A.; Dufourc, E. J.; Géan, J. Membrane Lipids Protected from Oxidation by Red Wine Tannins: A Proton NMR Study. *Biochimie* **2014**, *107* (Part A), 82–90. https://doi.org/10.1016/j.biochi.2014.07.008.

(98) Heckler, R. P.; Almeida, G. D.; Santos, L. B.; Borges, D. G. L.; Neves, J. P. L.; Onizuka, M. K. V.; Borges, F. A. P-Gp Modulating Drugs Greatly Potentiate the in Vitro Effect of Ivermectin against Resistant Larvae of *Haemonchus Placei*. *Vet. Parasitol.* **2014**, *205* (3–4), 638–645. https://doi.org/10.1016/j.vetpar.2014.08.002.

(99) Molento, M. B.; Lifschitz, A.; Sallovitz, J.; Lanusse, C.; Prichard, R. Influence of Verapamil on the Pharmacokinetics of the Antiparasitic Drugs Ivermectin and Moxidectin in Sheep. *Parasitol. Res.* **2004**, *92* (2), 121–127. https://doi.org/10.1007/s00436-003-1022-3.

(100) Molento, M. B.; Prichard, R. K. Effects of the Multidrug-Resistance-Reversing Agents Verapamil and CL 347,099 on the Efficacy of Ivermectin or Moxidectin against Unselected and Drug-Selected Strains of *Haemonchus Contortus* in Jirds (*Meriones Unguiculatus*). *Parasitol. Res.* **1999**, *85* (12), 1007–1011. https://doi.org/10.1007/s004360050673.

(101) Lespine, A.; Ménez, C.; Bourguinat, C.; Prichard, R. K. P-Glycoproteins and Other Multidrug Resistance Transporters in the Pharmacology of Anthelmintics: Prospects for Reversing Transport-Dependent Anthelmintic Resistance. *Int. J. Parasitol. Drugs Drug Resist.* **2012**, *2*, 58–75. https://doi.org/10.1016/j.ijpddr.2011.10.001.

(102) Lifschitz, A.; Suarez, V. H.; Sallovitz, J.; Cristel, S. L.; Imperiale, F.; Ahoussou, S.; Schiavi, C.; Lanusse, C. Cattle Nematodes Resistant to Macrocyclic Lactones: Comparative Effects of P-Glycoprotein Modulation on the Efficacy and Disposition Kinetics of Ivermectin and Moxidectin. *Exp. Parasitol.* **2010**, *125* (2), 172–178. https://doi.org/10.1016/j.exppara.2010.01.009.

(103) De Graef, J.; Demeler, J.; Skuce, P.; Mitreva, M.; Von Samson-Himmelstjerna, G.; Vercruysse, J.; Claerebout, E.; Geldhof, P. Gene Expression Analysis of ABC Transporters in a Resistant *Cooperia Oncophora* Isolate Following *in Vivo* and *in Vitro* Exposure to Macrocyclic Lactones. *Parasitology* **2013**, *140* (4), 499–508. https://doi.org/10.1017/S0031182012001849.

(104) Prichard, R. K.; Roulet, A. ABC Transporters and β-Tubulin in Macrocyclic Lactone Resistance: Prospects for Marker Development. *Parasitology* **2007**, *134* (8), 1123–1132. https://doi.org/10.1017/S0031182007000091.

(105) Xu, M.; Molento, M.; Blackhall, W.; Ribeiro, P.; Beech, R.; Prichard, R. Ivermectin Resistance in Nematodes May Be Caused by Alteration of P-Glycoprotein Homolog. *Mol. Biochem. Parasitol.* **1998**, *91* (2), 327–335. https://doi.org/10.1016/S0166-6851(97)00215-6.

(106) Yazaki, K. ABC Transporters Involved in the Transport of Plant Secondary Metabolites. *FEBS Lett.* **2006**, *580*, 1183–1191. https://doi.org/10.1016/j.febslet.2005.12.009.

(107) Kitagawa, S.; Nabekura, T.; Nakamura, Y.; Takahashi, T.; Kashiwada, Y. Inhibition of P-Glycoprotein Function by Tannic Acid and Pentagalloylglucose. *J. Pharm. Pharmacol.* **2007**, *59* (7), 965–969. https://doi.org/10.1211/JPP.59.7.0008.

(108) Chieli, E.; Romiti, N.; Rodeiro, I.; Garrido, G. *In Vitro* Modulation of ABCB1/P-Glycoprotein Expression by Polyphenols from *Mangifera Indica*. *Chem. Biol. Interact.* **2010**, *186* (3), 287–294. https://doi.org/10.1016/j.cbi.2010.05.012.

(109) Virkel, G.; Lifschitz, A.; Sallovitz, J.; Ballent, M.; Scarcella, S.; Lanusse, C. Inhibition of Cytochrome P450 Activity Enhances the Systemic Availability of Triclabendazole Metabolites in Sheep. *J. Vet. Pharmacol. Ther.* **2009**, *32* (1), 79–86. https://doi.org/10.1111/j.1365-2885.2008.01006.x.

(110) Benchaoui, H. A.; Mckellar, Q. A. Interaction between Fenbendazole and Piperonyl Butoxide: Pharmacokinetic and Pharmacodynamic Implications. *J. Pharm. Pharmacol.* **1996**, *48* (7), 753–759. https://doi.org/10.1111/j.2042-7158.1996.tb03965.x.

(111) Jones, L. M.; Flemming, A. J.; Urwin, P. E. NHR-176 Regulates Cyp-35d1 to Control Hydroxylation-Dependent Metabolism of Thiabendazole in *Caenorhabditis Elegans*. *Biochem. J.* **2015**, *466* (1), 37–44. https://doi.org/10.1042/BJ20141296.

(112) Virkel, G.; Lifschitz, A.; Sallovitz, J.; Pis, A.; Lanusse, C. Comparative Hepatic and Extrahepatic Enantioselective Sulfoxidation of Albendazole and Fenbendazole in Sheep and Cattle. *Drug Metab. Dispos.* **2004**, *32* (5), 536–544. https://doi.org/10.1124/dmd.32.5.536.
(113) Nebert, D. W.; Russell, D. W. Clinical Importance of the Cytochromes P450. *Lancet* **2002**, *360* (9340), 1155–1162. https://doi.org/10.1016/S0140-6736(02)11203-7.
(114) Hodek, P.; Trefil, P.; Stiborová, M. Flavonoids-Potent and Versatile Biologically Active Compounds Interacting with Cytochromes P450. *Chem. Biol. Interact.* **2002**, *139* (1), 1–21. https://doi.org/10.1016/S0009-2797(01)00285-X.
(115) Ma, Y. L.; Zhao, F.; Yin, J. T.; Liang, C. J.; Niu, X. L.; Qiu, Z. H.; Zhang, L. T. Two Approaches for Evaluating the Effects of Galangin on the Activities and MRNA Expression of Seven CYP450. *Mol. 2019, Vol. 24, Page 1171* **2019**, *24* (6), 1171. https://doi.org/10.3390/MOLECULES24061171.
(116) Bee, G.; Silacci, P.; Ampuero-Kragten, S.; Čandek-Potokar, M.; Wealleans, A. L.; Litten-Brown, J.; Salminen, J. P.; Mueller-Harvey, I. Hydrolysable Tannin-Based Diet Rich in Gallotannins Has a Minimal Impact on Pig Performance but Significantly Reduces Salivary and Bulbourethral Gland Size. *animal* **2017**, *11* (9), 1617–1625. https://doi.org/10.1017/S1751731116002597.
(117) Yao, H. T.; Chang, Y. W.; Lan, S. J.; Yeh, T. K. The Inhibitory Effect of Tannic Acid on Cytochrome P450 Enzymes and NADPH-CYP Reductase in Rat and Human Liver Microsomes. *Food Chem. Toxicol.* **2008**, *46* (2), 645–653. https://doi.org/10.1016/J.FCT.2007.09.073.
(118) Basheer, L.; Kerem, Z. Interactions between CYP3A4 and Dietary Polyphenols. *Oxid. Med. Cell. Longev.* **2015**, *2015* (1), 854015. https://doi.org/10.1155/2015/854015.
(119) Frazier, R. A.; Papadopoulou, A.; Mueller-Harvey, I.; Kissoon, D.; Green, R. J. Probing Protein-Tannin Interactions by Isothermal Titration Microcalorimetry. *J. Agric. Food Chem.* **2003**, *51* (18), 5189–5195. https://doi.org/10.1021/jf021179v.
(120) Frazier, R. A.; Papadopoulou, A.; Green, R. J. Isothermal Titration Calorimetry Study of Epicatechin Binding to Serum Albumin. *J. Pharm. Biomed. Anal.* **2006**, *41* (5), 1602–1605. https://doi.org/10.1016/j.jpba.2006.02.004.
(121) Dobreva, M. A.; Frazier, R. A.; Mueller-Harvey, I.; Clifton, L. A.; Gea, A.; Green, R. J. Binding of Pentagalloyl Glucose to Two Globular Proteins Occurs via Multiple Surface Sites. *Biomacromolecules* **2011**, *12* (3), 710–715. https://doi.org/10.1021/bm101341s.
(122) McRae, J. M.; Falconer, R. J.; Kennedy, J. A. Thermodynamics of Grape and Wine Tannin Interaction with Polyproline: Implications for Red Wine Astringency. *J. Agric. Food Chem.* **2010**, *58* (23), 12510–12518. https://doi.org/10.1021/JF1030967.
(123) Sun, Q.; He, J.; Yang, H.; Li, S.; Zhao, L.; Li, H. Analysis of Binding Properties and Interaction of Thiabendazole and Its Metabolite with Human Serum Albumin via Multiple Spectroscopic Methods. *Food Chem.* **2017**, *233*, 190–196. https://doi.org/10.1016/j.foodchem.2017.04.119.
(124) Stepniak, A.; Erdenebayar, B.; Biernacka, M.; Buczkowski, A.; Zavodnik, L.; Zavodnik, I.; Palecz, B. Calorimetric Studies of α-Cyclodextrin Inclusion Complexes with Carbendazim and Thiabendazole. *Phys. Chem. Liq.* **2020**, 1–8. https://doi.org/10.1080/00319104.2020.1737693.
(125) Ross, P. D.; Subramanian, S. Thermodynamics of Protein Association Reactions: Forces Contributing to Stability. *Biochemistry* **1981**, *20* (11), 3096–3102.
(126) Turnbull, W. B.; Daranas, A. H. On the Value of c: Can Low Affinity Systems Be Studied by Isothermal Titration Calorimetry? *J. Am. Chem. Soc.* **2003**, *125* (48), 14859–14866. https://doi.org/10.1021/JA036166S.
(127) Imran, I. Bin; Karonen, M.; Salminen, J.-P.; Engström, M. T. Modification of Natural Proanthocyanidin Oligomers and Polymers Via Chemical Oxidation under Alkaline Conditions. *ACS Omega* **2021**, *6*, 4726–4739. https://doi.org/10.1021/acsomega.0c05515.
(128) Salminen, J.-P.; Karonen, M. Chemical Ecology of Tannins and Other Phenolics: We Need a Change in Approach. *Funct. Ecol.* **2011**, *25* (2), 325–338. https://doi.org/10.1111/j.1365-2435.2010.01826.x.

(129) Engström, M. T.; Pälijärvi, M.; Salminen, J. P. Rapid Fingerprint Analysis of Plant Extracts for Ellagitannins, Gallic Acid, and Quinic Acid Derivatives and Quercetin-, Kaempferol- and Myricetin-Based Flavonol Glycosides by UPLC-QqQ-MS/MS. *J. Agric. Food Chem.* **2015**, *63* (16), 4068–4079. https://doi.org/10.1021/acs.jafc.5b00595.

(130) Engström, M. T.; Pälijärvi, M.; Fryganas, C.; Grabber, J. H.; Mueller-Harvey, I.; Salminen, J. P. Rapid Qualitative and Quantitative Analyses of Proanthocyanidin Oligomers and Polymers by UPLC-MS/MS. *J. Agric. Food Chem.* **2014**, *62* (15), 3390–3399. https://doi.org/10.1021/jf500745y.

(131) Gea, A.; Stringano, E.; Brown, R. H.; Mueller-Harvey, I. In Situ Analysis and Structural Elucidation of Sainfoin (*Onobrychis Viciifolia*) Tannins for High-Throughput Germplasm Screening. *J. Agric. Food Chem.* **2011**, *59* (2), 495–503. https://doi.org/10.1021/JF103609P.

(132) Hellström, J.; Sinkkonen, J.; Karonen, M.; Mattila, P. Isolation and Structure Elucidation of Procyanidin Oligomers from Saskatoon Berries (*Amelanchier Alnifolia*). *J. Agric. Food Chem.* **2007**, *55* (1), 157–164. https://doi.org/10.1021/JF062441T.

(133) O'Kennedy, S. J.; de Villiers, A.; Brand, D. J.; Gerber, W. J. A Variable Temperature 1H NMR and DFT Study of Procyanidin B2 Conformational Interchange. *Struct. Chem.* **2018**, *29* (5), 1551–1564. https://doi.org/10.1007/S11224-018-1153-X.

(134) Gu, L.; Kelm, M. A.; Hammerstone, J. F.; Beecher, G.; Holden, J.; Haytowitz, D.; Prior, R. L. Screening of Foods Containing Proanthocyanidins and Their Structural Characterization Using LC-MS/MS and Thiolytic Degradation. *J. Agric. Food Chem.* **2003**, *51* (25), 7513–7521. https://doi.org/10.1021/jf034815d.

(135) Karchesy, J. J.; Foo, L. Y.; Barofskv, E.; Arbogast, B.; Barofsky, D. F. Negative-Ion Fast-Atom-Bombardment Mass Spectrometry of Procyanidin Oligomers. *J. Wood Chem. Technol.* **1989**, *9* (3), 313–331. https://doi.org/10.1080/02773818908050302.

(136) Friedrich, W.; Eberhardt, A.; Galensa, R. I. Investigation of Proanthocyanidins by HPLC with Electrospray Ionization Mass Spectrometry. *Eur. Food Res. Technol.* **2000**, *200*, 56–64. https://doi.org/10.1007/S002170050589.

(137) Sui, Y.; Zheng, Y.; Li, X.; Li, S.; Xie, B.; Sun, Z. Characterization and Preparation of Oligomeric Procyanidins from *Litchi Chinensis* Pericarp. *Fitoterapia* **2016**, *112*, 168–174. https://doi.org/10.1016/J.FITOTE.2016.06.001.

(138) Karonen, M.; Imran, I. Bin; Engström, M. T.; Salminen, J. P. Characterization of Natural and Alkaline-Oxidized Proanthocyanidins in Plant Extracts by Ultrahigh-Resolution UHPLC-MS/MS. *Molecules* **2021**, *26* (7), 1873. https://doi.org/10.3390/molecules26071873.

(139) Karonen, M.; Loponen, J.; Ossipov, V.; Pihlaja, K. Analysis of Procyanidins in Pine Bark with Reversed-Phase and Normal-Phase High-Performance Liquid Chromatography-Electrospray Ionization Mass Spectrometry. *Anal. Chim. Acta* **2004**, *522* (1), 105–112. https://doi.org/10.1016/j.aca.2004.06.041.

(140) Lin, L. Z.; Sun, J.; Chen, P.; Monagas, M. J.; Harnly, J. M. UHPLC-PDA-ESI/HRMSnprofiling Method to Identify and Quantify Oligomeric Proanthocyanidins in Plant Products. *J. Agric. Food Chem.* **2014**, *62* (39), 9387–9400. https://doi.org/10.1021/jf501011y.

(141) Li, S.; Xiao, J.; Chen, L.; Hu, C.; Chen, P.; Xie, B.; Sun, Z. Identification of A-Series Oligomeric Procyanidins from Pericarp of Litchi Chinensis by FT-ICR-MS and LC-MS. *Food Chem.* **2012**, *135* (1), 31–38. https://doi.org/10.1016/j.foodchem.2012.04.039.

(142) Frazier, R. A.; Deaville, E. R.; Green, R. J.; Stringano, E.; Willoughby, I.; Plant, J.; Mueller-Harvey, I. Interactions of Tea Tannins and Condensed Tannins with Proteins. *J. Pharm. Biomed. Anal.* **2010**, *51* (2), 490–495. https://doi.org/10.1016/j.jpba.2009.05.035.

(143) Tellinghuisen, J. Statistical Error in Isothermal Titration Calorimetry. *Methods Enzymol.* **2004**, *383* (1996), 245–282. https://doi.org/10.1016/S0076-6879(04)83011-8.

(144) Tellinghuisen, J. Stupid Statistics! *Methods in Cell Biology*. Academic Press January 1, 2008, pp 737–780. https://doi.org/10.1016/S0091-679X(07)84023-4.

(145) Poncet-Legrand, C.; Gautier, C.; Cheynier, V.; Imberty, A. Interactions between Flavan-3-Ols and Poly(L-Proline) Studied by Isothermal Titration Calorimetry: Effect of the Tannin Structure. *J. Agric. Food Chem.* **2007**, *55* (22), 9235–9240. https://doi.org/10.1021/jf071297o.

(146) Murray, N. J.; Williamson, M. P.; Lilley, T. H.; Haslam, E. Study of the Interaction between Salivary Proline-rich Proteins and a Polyphenol by 1H-NMR Spectroscopy. *Eur. J. Biochem.* **1994**, *219* (3), 923–935. https://doi.org/10.1111/j.1432-1033.1994.tb18574.x.

(147) Charlton, A. J.; Baxter, N. J.; Khan, M. L.; Moir, A. J. G.; Haslam, E.; Davies, A. P.; Williamson, M. P. Polyphenol/Peptide Binding and Precipitation. *J. Agric. Food Chem.* **2002**, *50* (6), 1593–1601. https://doi.org/10.1021/jf010897z.

(148) Simon, C.; Barathieu, K.; Laguerre, M.; Schmitter, J. M.; Fouquet, E.; Pianet, I.; Dufourc, E. J. Three-Dimensional Structure and Dynamics of Wine Tannin-Saliva Protein Complexes. A Multitechnique Approach. *Biochemistry* **2003**, *42* (35), 10385–10395. https://doi.org/10.1021/bi034354p.

(149) Cala, O.; Pinaud, N.; Simon, C.; Fouquet, E.; Laguerre, M.; Dufourc, E. J.; Pianet, I. NMR and Molecular Modeling of Wine Tannins Binding to Saliva Proteins: Revisiting Astringency from Molecular and Colloidal Prospects. *FASEB J.* **2010**, *24* (11), 4281–4290. https://doi.org/10.1096/fj.10-158741.

(150) Stamm, H.; Jäckel, H. Relative Ring-Current Effects Based on a New Model for Aromatic-Solvent-Induced Shift. *J. Am. Chem. Soc.* **1989**, *111* (17), 6544–6550. https://doi.org/10.1021/ja00199a010.

(151) Scheidt, H. A.; Pampel, A.; Nissler, L.; Gebhardt, R.; Huster, D. Investigation of the Membrane Localization and Distribution of Flavonoids by High-Resolution Magic Angle Spinning NMR Spectroscopy. *Biochim. Biophys. Acta - Biomembr.* **2004**, *1663* (1–2), 97–107. https://doi.org/10.1016/j.bbamem.2004.02.004.

(152) Lumsden, M. D.; Wasylishen, R. E.; Eichele, K.; Penner, G. H.; Power, W. P.; Curtis, R. D.; Schindler, M. Carbonyl Carbon and Nitrogen Chemical Shift Tensors of the Amide Fragment of Acetanilide and N-Methylacetanilide. *J. Am. Chem. Soc.* **1994**, *116* (4), 1403–1413. https://doi.org/10.1021/ja00083a028.

(153) Williamson, M. P. Using Chemical Shift Perturbation to Characterise Ligand Binding. *Prog. Nucl. Magn. Reson. Spectrosc.* **2013**, *73*, 1–16. https://doi.org/10.1016/j.pnmrs.2013.02.001.

TURUN
YLIOPISTO
UNIVERSITY
OF TURKU

Painosalama, Turku, Finland 2025

ISBN 978-952-02-0275-0 (PRINT)
ISBN 978-952-02-0276-7 (PDF)
ISSN 0082-7002 (Print)
ISSN 2343-3175 (Online)